Supplied by:
WINDSOR SCIENTIFIC LTD
264 Argyll Avenue, Slough Trading Estate
Slough, Berkshire, SL1 4HE
Telephone: 01753-822522
Facsimile: 01753-822002
E-mail: sales@windsorscientific.co.uk
Web: www.windsorscientific.co.uk

© Nanosurf AG, 2007
Printed in Switzerland

Nanosurf AG
Grammetstrasse 14
CH-4410 Liestal

E-Mail
info@nanosurf.com

World Wide Web
www.nanosurf.com

Nanosurf® AFM Extended Sample Kit

User Manual

User Manual

Nanosurf AFM Extended Sample Kit

Version 1.4

Table of contents

"Nanosurf" and the Nanosurf Logo are trademarks of Nanosurf AG,
registered and/or otherwise protected in various countries.
Copyright © August 2010, Nanosurf AG, Switzerland.

Table of contents

CHAPTER 1: The AFM Extended Sample Kit 8

CHAPTER 2: An introduction to atomic force microscopy 12

2.1: Introduction **12**

2.2: The AFM Setup **13**

2.2.1: The Force Sensor 14

2.2.2: The Deflection Detector 16

2.2.3: The PID Feedback System 16

2.2.4: AFM Operating Modes 20

2.2.5: The Scanning System and Data Collection 21

CHAPTER 3: Chip Structure in Silicon 24

3.1: Measurements **25**

3.1.1: Image Acquisition 25

3.1.2: Image Analysis 25

3.1.3: Integrated Circuit Technology 28

3.1.4: Transistors 28

3.1.5: Integrated circuit production 30

3.2: Sample Maintenance **32**

CHAPTER 4: CD Stamper 36

4.1: Measurement **36**

4.1.1: Image Acquisition 36

4.1.2: Image Analysis 37

4.2: Optical Data Storage **38**

4.2.1: Manufacturing 39

4.2.2: Data Encoding 39

4.3: Sample Maintenance **41**

CHAPTER 5: Gold Clusters 44

5.1: Measurement **44**

5.1.1: Image Acquisition 44

5.1.2: Image Analysis 45

5.2: Fabrication of the Gold Clusters **47**

CHAPTER 6: Nanotubes 50

6.1: Measurement **50**

6.1.1: Image Acquisition 50

6.1.2: Image Analysis 51

6.2: Carbon Nanotubes **54**

CHAPTER 7: Glass Beads 58

7.1: Measurements **58**

7.1.1: Sample Preparation 58

7.1.2: Image Acquisition 59

7.1.3: Image Analysis 61

7.2: Relevance of the Glass Beads **63**

CHAPTER 8: Staphylococcus aureus 66

8.1: Measurement **66**

8.1.1: Image Acquisition 66

8.1.2: Image Analysis 67

CHAPTER 9: Microstructure 72

9.1: Measurement **72**

9.1.1: Image Acquisition 72

9.1.2: Image Analysis 72

9.2: Microfabrication **75**

CHAPTER 10: PS/PMMA Thin Film 78

10.1: Measurement **78**

10.1.1: Image Acquisition 78

10.1.2: Image Analysis 80

10.2: Relevance of Lateral Force measurements **82**

CHAPTER 11: Skin Cross-Section 86

11.1: Measurement **86**

11.1.1: Image Acquisition 86

11.1.2: Image Analysis 88

11.2: Biological Samples **90**

CHAPTER 12: Aluminum Foil 92
12.1: Measurements 92
12.1.1: Image Acquisition 92
12.1.2: Image Analysis 93
12.2: Bulk Foil Production 96
12.3: Sample Maintenance 97

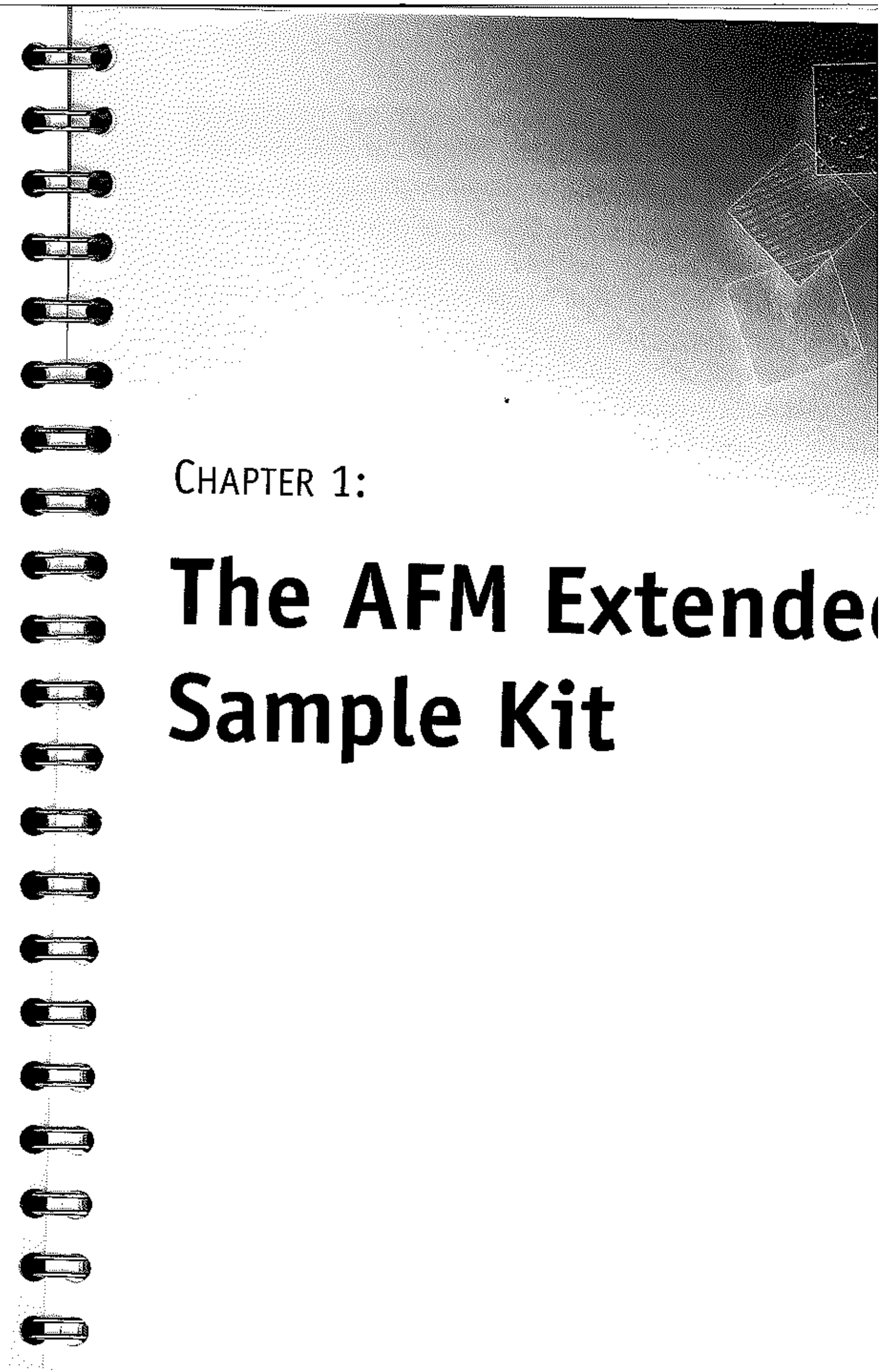

CHAPTER 1:

The AFM Extende[d] Sample Kit

Chapter 1: The AFM Extended Sample Kit

The AFM Extended Sample Kit shown in *Figure 1-1: AFM Extended Sample Kit* contains ten samples selected from various disciplines, tools to handle them, and a manual to guide the student through the investigation of each one. Each sample was specifically designed to emphasize interesting features of the sample itself and to highlight various aspects of the AFM. Some of the samples have the additional quality of representing actual current uses of AFM in the respective fields of science. This manual is intended to serve as a collection of suggestions rather than as a 'how-to' manual. By exploring the samples, there is freedom to make mistakes and to learn which conditions produce desired results and which do not. It is not necessary to read the chapters in this manual in numerical order.

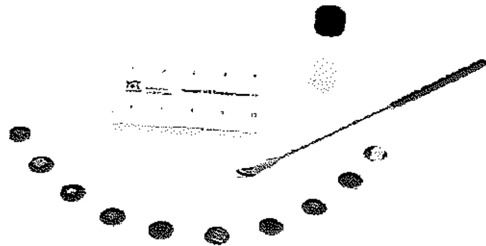

Figure 1-1: AFM Extended Sample Kit

The manual starts with a brief introduction to atomic force microscopy (AFM), followed by a description of the samples contained in the AFM Extended Sample Kit. The samples introduce the following topics:

1. Chip Structure in Silicon: Setting the optimum PID feedback gains
2. CD Stamper: Using the distance and length tool.
3. Gold clusters: Doing roughness analysis.
4. Nanotubes: Choosing the optimum Set point.
5. Glass beads: Estimating the tip radius.
6. Staphylococcus Aureus: Approaching a non reflective sample.

7. Microstructure: Setting the correct vibration amplitude.
8. PS/PMMA Thin Film: Performing phase contrast and lateral force.
9. Skin Cross Section: Positioning the tip at specific positions.
10. Aluminum Foil: Estimating data processing artefacts.

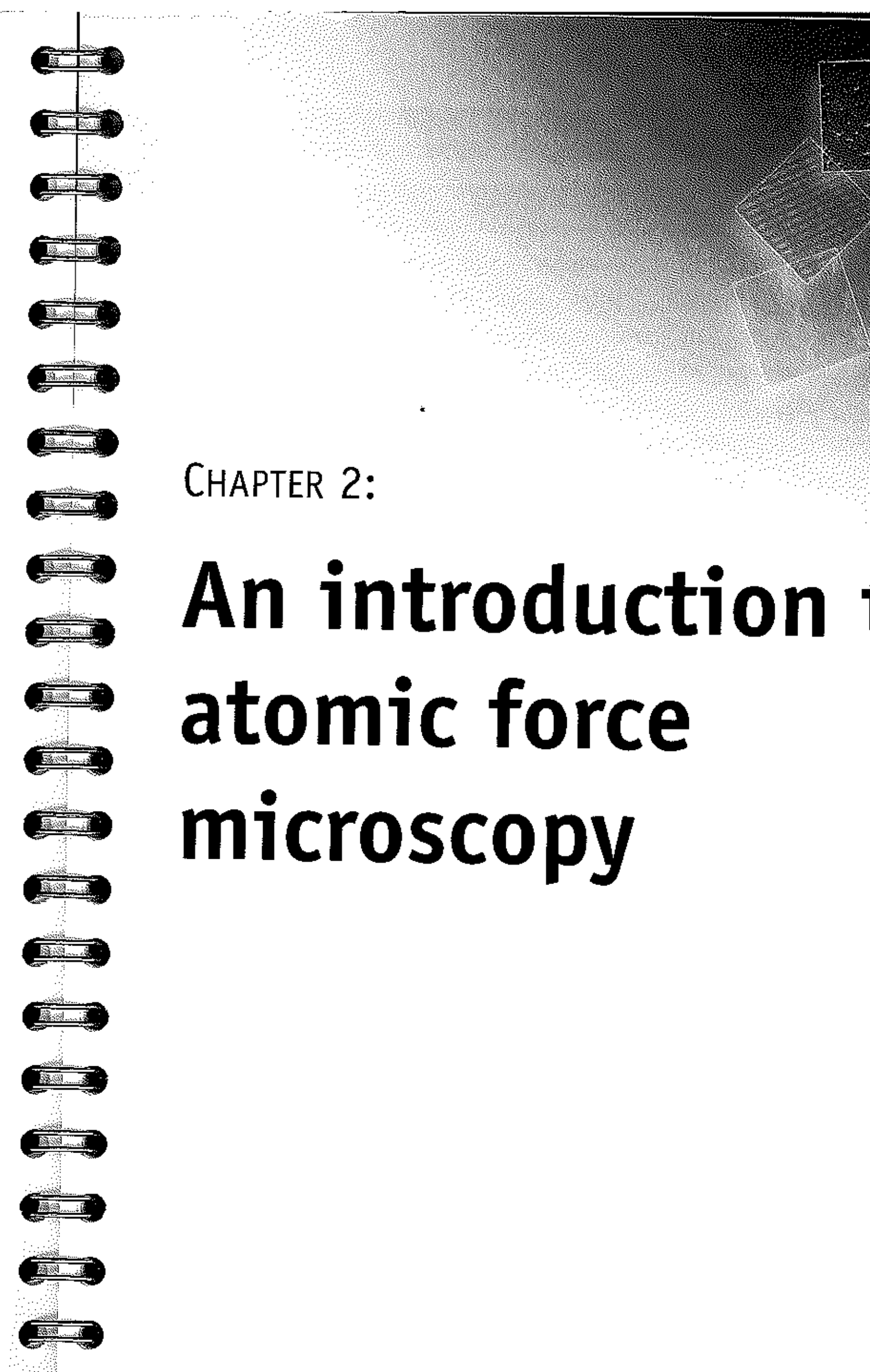

CHAPTER 2:

An introduction t atomic force microscopy

CHAPTER 2: An introduction to atomic force microscopy

2.1: Introduction

In 1986, Gerd Binnig and Heinrich Rohrer won the Nobel Prize in Physics for the invention of the scanning tunnelling microscope (STM) and the fact that it could achieve atomic resolution. They observed that if they held a metallic tip of 10 angstrom above a conductive surface, they could measure a tunnelling current in the order of a nanoampere. When the tip was then scanned over the conducting sample, the topography of the surface could be plotted by measuring the distance-dependent tunnelling current. The STM was a revolution in the field of high-resolution microscopy, however, this technique could only be used to image conducting samples.

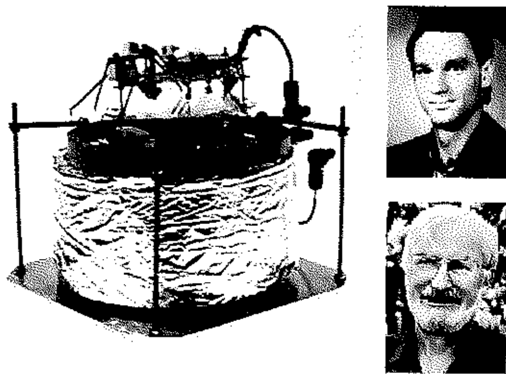

Figure 2-1: First STM. First STM (left) invented by Binnig (top) and Rohrer (bottom) in 1981. Images courtesy of IBM.

New scanning probe microscopes (SPM) based on the STM principle have therefore been invented. Among those the most promising is the atomic force microscope (AFM). The success of AFM is due to its capability to achieve atomic resolution and to simultaneously measure topography and other force-related material properties. AFM can also be used to image a huge variety of samples which of course do not need to be electrical conductors and could also be used in different environments like gas, vacuum and liquid.

The basic principle of AFM is very simple. The AFM detects the force interaction between a sample and a very tiny tip (<10 nm radius) mounted on a

cantilever. The force interaction between sample and tip is related to the deflection of the cantilever, i.e. the more the tip presses into the sample the greater the deflection of the cantilever and the greater the force exercised on the sample. A regulating feedback system tries to keep the deflection of the cantilever and thus the force interaction constant. Therefore the cantilever is moved away from the surface or towards the surface depending on how the force changes. This movement is then recorded as topography signal when the tip is scanned over a sample. The topography can thus also be interpreted as a map of equal forces. It is thus possible to detect any kind of force as long as the tip is sensitive enough, i.e. as long as the force interaction induces a measurable deflection of the cantilever. Hence not only interatomic forces but also long range forces like magnetic force and electrostatic force can be detected.

2.2: The AFM Setup

Independently of the type of tip–sample interaction an AFM basically consist of five major parts shown in *Figure 2-2: AFM Setup* (page 14) and described in the following sections:

1. A force sensor, which is basically a sharp tip (< 10 nm) mounted on a sensitive cantilever.
2. A scanner which moves the sample or the sensor in order to probe the sample surface.
3. A sensor which detects the cantilever deflection, for example a laser deflection system or piezoresistive system.
4. A feed-back system which regulates the force interaction.
5. Controller electronics which records movements, controls the feedback loop and sends the measured data to ta personal computer software.

Even if these parts are present in every AFM, their implementation can differ substantially. However a common point to all AFM is the force sensor, also called AFM probe. It is plausible that the results strongly depend on the sharpness of the tip and the spring constant of the cantilever. This will be the subject of *Section 2.2.1: The Force Sensor* (page 14). The deflection detection system needs to be very sensitive and can be implemented in different ways

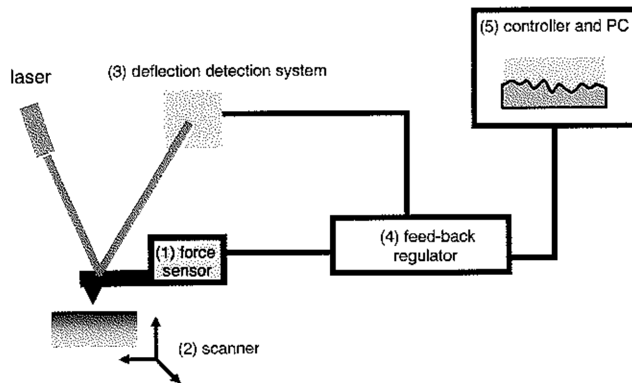

Figure 2-2: AFM Setup. The five components of an AFM setup

which will be discussed in *Section 2.2.2: The Deflection Detector* (page 16). The feedback system will be described in *Section 2.2.3: The PID Feedback System* (page 16). The AFM can be operated in different modes which will be discussed in *Section 2.2.4: AFM Operating Modes* (page 20). Finally, *Section 2.2.5: The Scanning System and Data Collection* (page 21) will deal with the positioning or scanning system which needs to provide nanometer resolution.

2.2.1: The Force Sensor

AFM probes are typically micro-fabricated. The single-leg or V-shaped cantilevers are usually made out of silicon, silicon-dioxide or silicon-nitride. Typical cantilevers are several hundred micrometers long, several tens of micrometers wide and around one micrometer thick. For silicon these dimensions will result in spring constants between 0.1 and 1 N/m and resonance frequencies between 10 and 100 kHz.

Thanks to recent developments in microtechnology it is possible to fabricate cantilevers with integrated sharp tips. It is important to keep in mind that the quality of the tip, i.e. the shape of the tip, determines the quality of the measurement. The critical dimensions of an AFM tip are its aspect ratio (height/width), the radius of curvature (sharpness) and its material. The ideal tip has a high aspect ratio, a small radius of curvature and is made of an extremely hard material. The shape of the tip is of great importance when it comes to the

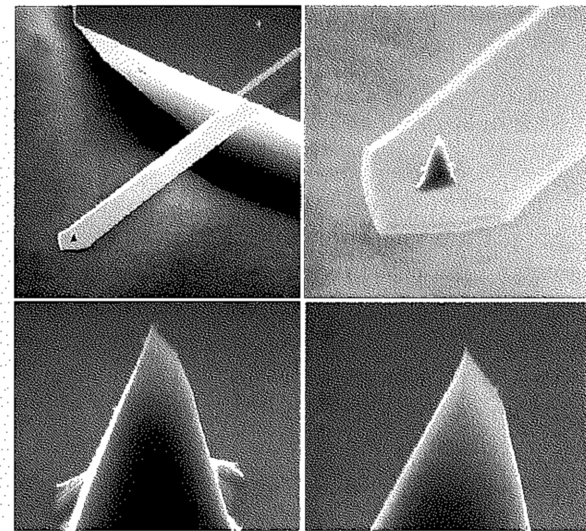

Figure 2-3: AFM Probe. Tip and cantilever of an AFM probe.

interpretation of the measurement. Due to the fact that not only the very apex of the tip but also its side walls interact with the sample during scanning, the measured image is always a convolution between the tip shape and the sample. Therefore it is important that the feature size of the sample and their aspect ratios are some orders bigger than the radius of curvature and aspect ratio of the tip, respectively.

In AFM, the force sensor needs to meet the two following requirements:

1. Contact Mode (see *Section 2.2.4: AFM Operating Modes* (page 20)): The spring constant of the cantilever needs to be small, such that the cantilever can be sufficiently deflected and the deflection can be detected. Ideally the spring constant should be smaller than the interatomic spring constant, which is about 10 N/m.
2. Dynamic mode (see *Section 2.2.4: AFM Operating Modes* (page 20)): The portion of perturbation transmitted to the cantilever is given by $a_{trans} = a_0(f_0/f_{ex})^2$, where f_{ex} is the excitation vibration frequency with amplitude a_0 and f_0 is the resonance frequency. It is therefore usual to use

cantilevers with high resonance frequency in order to avoid low frequency acoustic or mechanic perturbation such as building vibrations.

2.2.2: The Deflection Detector

Another critical part of the AFM is the deflection measurement system. Ideally, the sensing system must be able to measure the deflection of the cantilever with angstrom resolution and must not perturb the cantilever in any way. The most used detection system is therefore an optical technique based on the reflection of a laser beam on the cantilever. The idea of the technique is shown in *Figure 2-2: AFM Setup* (page 14). A laser beam is focused on the very end of the cantilever which reflects it back on a segmented photo diode. The deflection angle of the cantilever is thereby enhanced, i.e. a small displacement of the cantilever results in a bigger displacement of the reflected laser beam on the photo diode. The further away the diode the bigger this mechanical amplification. However the photo diode can't be placed to far away because of external perturbation. One reason for that is that the laser deflection method is sensitive to the ambient light, the light reflected by the sample or the cantilever and other possible sources of light. The optical detection system allows measurement of deflections below one angstrom.

Other cantilever deflection detection techniques, which will not be discussed here, are:

- Interferometric optical systems
- Piezoresistive detection

2.2.3: The PID Feedback System

Before starting any AFM measurement it is necessary to understand how the feedback regulation system works. This regulation enables the acquisition of an AFM image. As described previously, the cantilever deflection is detected by a sensor. This position is then compared to a set-point, i.e. a constant value of cantilever deflection chosen by the user. As the deflection of the cantilever is directly related to the tip–sample interaction force, the set point is usually given in Newton (N). Typical forces are in the nN range. The difference between the actual interaction force and the desired force is called the error signal ΔS. This

error signal is then used to move the tip or sample to a distance where the cantilever has the desired deflection. This movement is then plotted in function of the lateral position of the tip and is the so-called topography. The goal of the feedback system is to minimize the error in a very fast manner so that the measured topography corresponds to the real topography of the sample. Therefore the error signal must be amplified by a PID controller (Proportional Integral Differential). A schematic representation of the feed-back system is shown in *Figure 2-4: PID controller.*

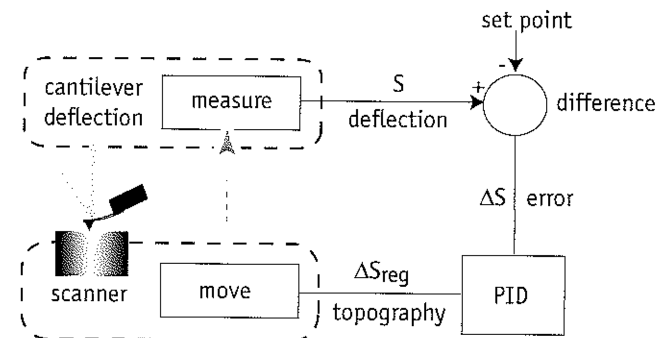

Figure 2-4: PID controller

As the name suggests, the PID controller has three domains of action:

1. Proportional Gain
2. Integral Gain
3. Differential Gain

These three gains can be set individually and define how fast and in which manner the error is minimized and the therefore how good the topography of the sample is reproduced in the measurement. Thus it is important to understand its characteristics. To illustrate the effect of the PID gains consider the following experiment.

A step signal from 0 to 1 will be measured (see *Figure 2-5: Step* (page 18)). The goal is to reproduce the rectangular step as precisely as possible. Hence the PID gains must be adjusted. *Figure 2-6: P-Gain* (page 18) shows the result when only the proportional gain (P) is turned up. The topography shows a long rise time

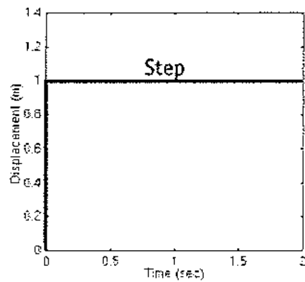

Figure 2-5: Step

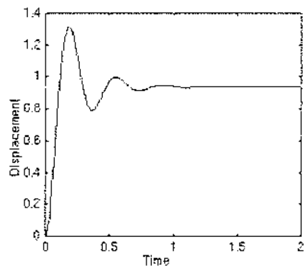

Figure 2-6: P-Gain

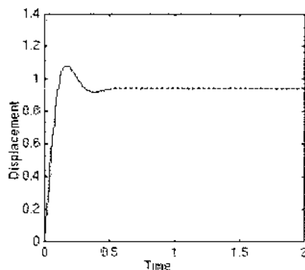

Figure 2-7: PD-Gain

(slope), an overshoot (peak) and a settling time (wobbles). As next the differential gain (D) will be turned up in addition to P. It can be seen in *Figure 2-7: PD-Gain* (page 18) that the derivative gain reduces both the overshoot and

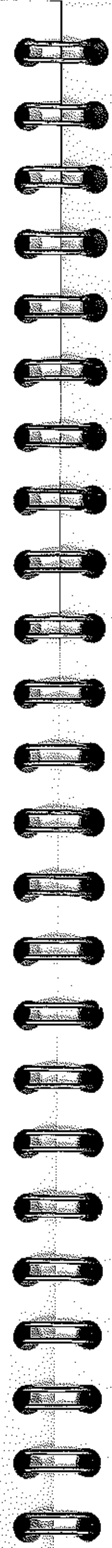

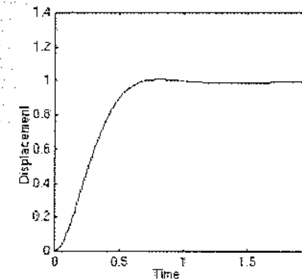

Figure 2-8: PI-Gain

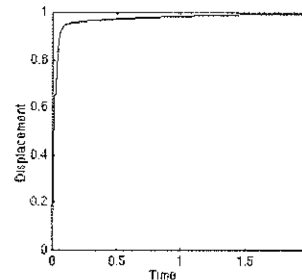

Figure 2-9: PID-Gain

the settling time, and had little effect on the rise time. In order to see the influence of the Integral gain (I) the D gain is turned down and the I gain up. As can be observed in *Figure 2-8: PI-Gain* the I controller further reduced the overshoot and decreased the settling time.

The response is much smoother now, albeit with an increased rising time. When the P, I and D gains are combined in an appropriate way it is possible to obtain the response shown in *Figure 2-9: PID-Gain* with no overshoot, short rise time, and short settling time.The correct PID settings are sample dependent and have to be determined for each measurement.

2.2.4: AFM Operating Modes

The AFM can be operated in different modes. This depends on the sample and on the information one would like to acquire. Among several modes here only the most common ones are discussed: contact, non contact and dynamic mode.

Static Mode

This mode is the most basic mode which was also the first real mode in which AFMs were operated. The tip is always in contact with the sample while probing the surface. Thereby the deflection of the cantilever and thus the interaction force is set by the user (set-point). The feedback regulator maintains this set-point by moving the scanner in the direction vertical to the sample. This movement generated by the regulation is then plotted as topography of the sample. The major parameter to set in this mode is the interaction force. This must be set to a minimum value, such that the tip is just in contact with the surface. The inconvenience of this method is that the tip might easily be contaminated or broken and that sticky samples can not be imaged correctly.

Dynamic Mode

Dynamic mode is probably the most used mode nowadays. The cantilever is oscillated. Hence the tip is touching the surface periodically. The contact with the surface attenuates the oscillation amplitude. The feedback regulates this attenuation compared to the desired set-point. Ideally the damping of the amplitude is related to the tip–sample interaction force which is therefore defined with the set-point. The set-point of this mode is given by the percentage of damped amplitude compared to the undamped amplitude, i.e. a set-point of 100% gives no interaction and a set-point of 60% means that the 40% of the vibration energy is lost in the interaction between tip and sample. As in contact mode, the goal is to keep the interaction as small as possible in order to avoid damage or contamination of the tip. In this case this means that the set-point needs to be as near to 100% as possible.

The oscillation amplitude is also an important parameter. Generally the oscillation amplitude has to be in the order of the features that have to be observed, i.e. large features need large amplitudes and tiny features need a small

amplitude. In order to measure tiny features on large features small amplitude and slow scan speeds are recommended.

The achievable resolution of the dynamic mode is comparable to the contact mode. However, due to the fact that the tip is only periodically in contact with the sample, the tip is less damaged and the lateral sticky forces are negligible.

2.2.5: The Scanning System and Data Collection

The scanning system of the AFM must be capable of placing the tip with a subatomic resolution, which is needed in order to image the sample with atomic resolution.

The movement of the tip or sample in the three axes can be realized in several ways. There are different implementations, e.g. piezoelectric, electromagnetic etc. As described in *Section 2.2.3: The PID Feedback System* (page 16), the topography image is generated by the feedback system which moves the scanner. This motion data is sent to the PC software through the AFM controller, usually line by line. The software combines the lines to a three-dimensional image where the height is usually represented with a color code.

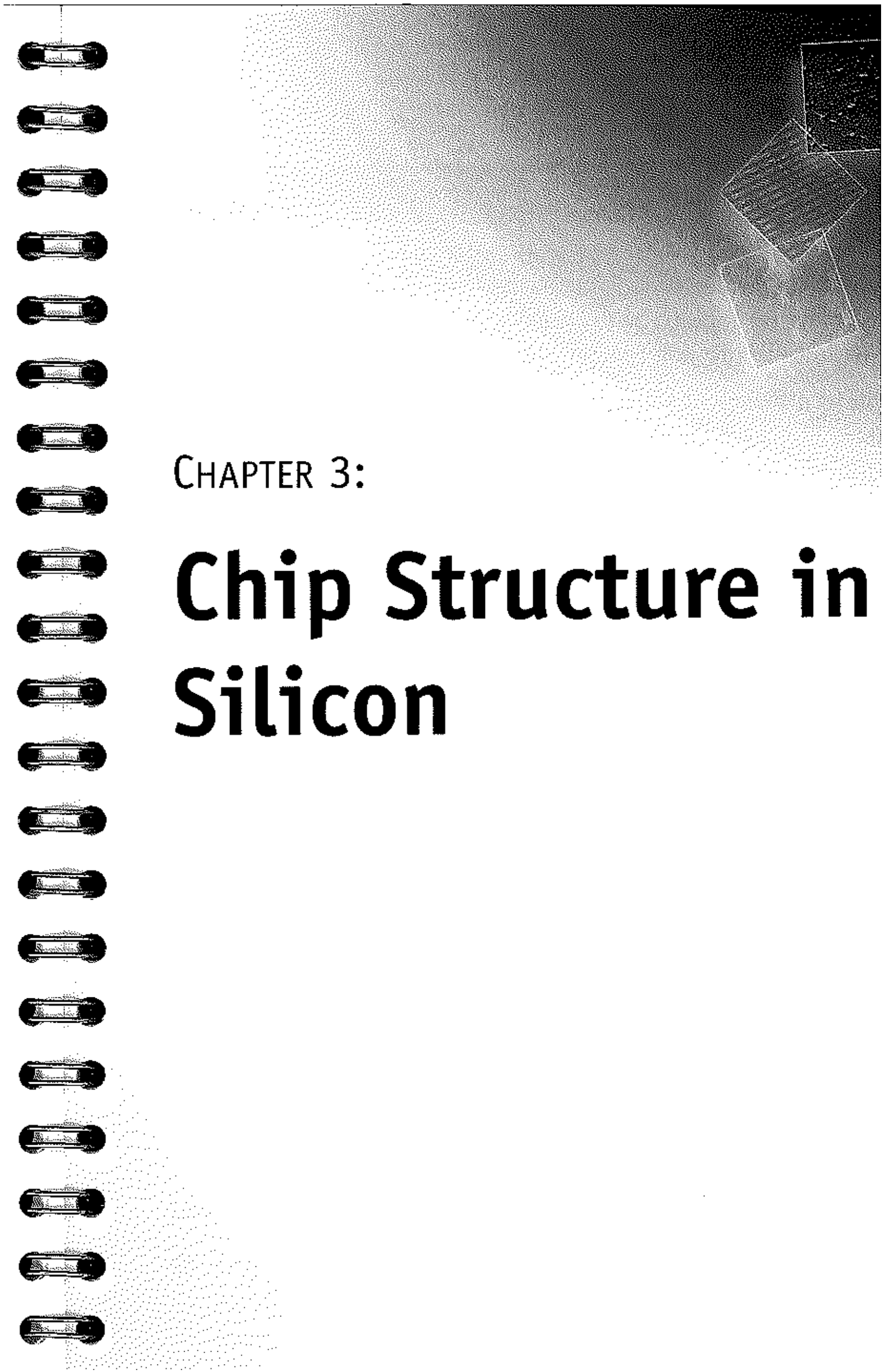

CHAPTER 3:

Chip Structure in Silicon

CHAPTER 3: Chip Structure in Silicon

The characterization of chips, also known as Integrated Circuits (ICs), is an important application of AFM technology. The dimensions of the structures in these circuits are decreasing rapidly, and no other tool is able to characterize these dimensions without destroying the sample.

This particular chip is a Switched Capacitor Array (SCA) chip. SCA chips are custom-made silicon chips which can sample an analog input signal at high speed (in this chip up to 950 GHz), but can then be read out at lower speeds. SCA chips contain regular structures and relatively deep trenches (see *Figure 3-1: The SCA Chip Structure*). The SCA chip is almost entirely covered with top metal (orange parts in *Figure 3-1: The SCA Chip Structure*, right). The left part with the small black rectangles (holes from the production process) is a data line that carries the input signals to the storage cells. The dark lines between the orange parts are separations between the top metal elements. The small orange squares that extend into the broad central separation are connections to the underlying metal layer. The L-shaped elements are connections to the underlying capacitors that store the recorded signals.

In the instruction given below, we will focus on the function and proper feedback settings of the Z-controller. The SCA sample is however also ideal for learning how the height measurement in the AFM works.

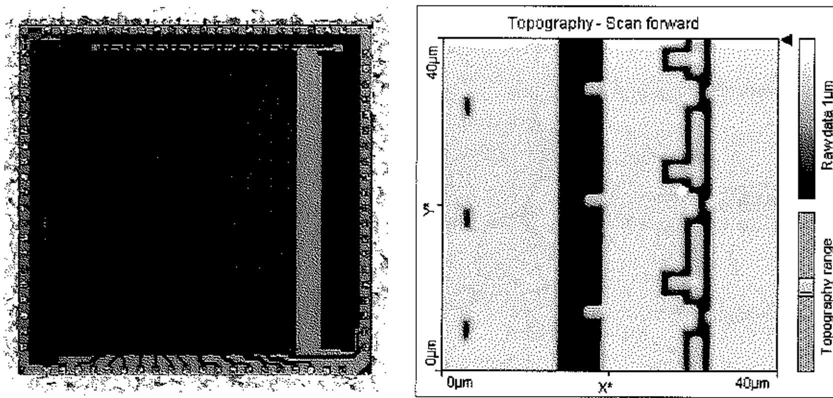

Figure 3-1: The SCA Chip Structure. (Left) Macroscopic overview. (Right) AFM image taken at the center of the chip (40-µm scan range; optimized settings).

3.1: Measurements

3.1.1: Image Acquisition

1. Set a large scan range, somewhere between 10 and 80 µm.
   The chip structure can be clearly seen at this size.
2. Approach the reflective part at the center of the sample.
   This is the section that contains the most interesting structures of the chip. Note the well-ordered, repeating pattern. The height of the structures (or rather: the depth of the trench) is approximately 1.6 µm.

3.1.2: Image Analysis

Since the chip structures are so well defined, this sample is conducive to testing the effects of your instrument's integral gain setting. Note that some systems have more than one type of gain setting. If your system has just one gain setting, it is the so-called "Integral" gain.

CAUTION

Excessively high or low gains can result in damaged to the tip. Monitor your system carefully when adjusting the gains.

Optimize your gain settings

- If you have not already done so, make sure your gains are set to levels that produce reasonable images.
  The line trace in *Figure 3-2: Optimized Gain* represents well optimized gain settings; the tip is accurately tracking the topography of the SCA sample.

Lowering the gain

- Lower the integral gain well below the optimal setting.
  As you lower the gain, the feedback loop will not work quickly enough to provide high resolution. Note the poorly defined edges in *Figure 3-3: Low Gain*. At a lowered gain, the feedback loop is not responding quickly enough to respond to changes in height.

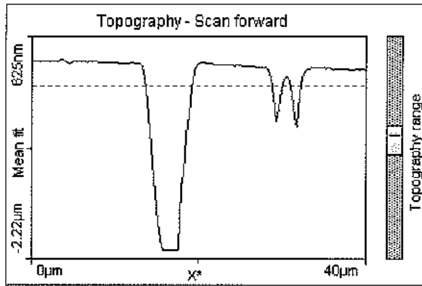

Figure 3-2: Optimized Gain. Optimized gain setting for SCA chip structure.

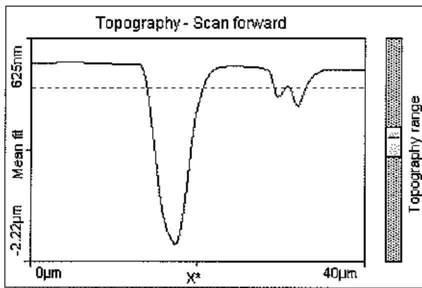

Figure 3-3: Low Gain. The feedback loop is not responding quickly enough.

Raising the gain

- Gradually raise the gain to well above the optimal settings.

  At some point, the Z-controller will start to overcompensate for feedback errors when the tip encounters steps in the sample. This overcompensation is also called overshoot.

Overshoot and Undershoot

When the gain settings are increased further, the controller will react to this overshoot by undershooting; the undershoot will be less than the overshoot. These overreactions initiate an oscillation that eventually subsides. The frequency of this oscillation is either the mechanical resonance frequency of the scanner or the resonance frequency of the cantilever itself.

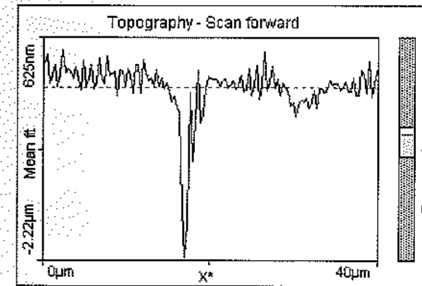

Figure 3-4: High Gain. Oscillating signal when gain is set too high.

At even higher gains, the oscillation will no longer subside. Instead, it will steadily increase, most likely resulting in damage to the cantilever tip. The oscillation should be visible in both the topography and the error signal (deflection or amplitude, depending on the measurement mode) images.

Be sure to monitor your system for indications that the controller is becoming unstable. First it will overshoot, and then it will "ring", which is represented by a vibration with decreasing amplitude at the step edges. Additionally, the error signal (in this case the cantilever deflection) will start to increase again.

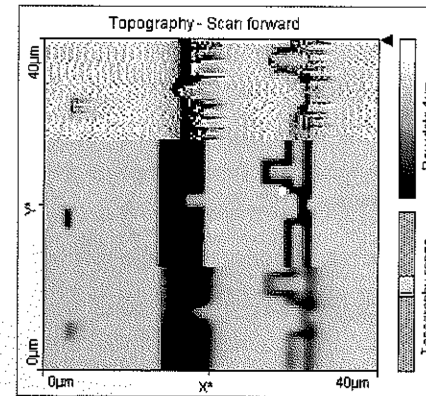

Figure 3-5: SCA chip structure imaged at different integral gain settings. In the lowest region of the image, the gain is too low; at the center, it is optimized; at the top, it is too high.

3.1.3: Integrated Circuit Technology

An integrated circuit (IC) is a single chip of semiconducting material (usually Silicon) on which all the functional elements (transistors, capacitors, wiring, and contacts) of an electronic circuit are integrated.

3.1.4: Transistors

The transistors are the enabling parts of many integrated circuits. In analog circuits, transistors are used as amplifiers, in which a small current or voltage controls a much larger current or voltage. In digital circuits, a voltage is used to switch a current on or off.

Transistors are generally made from a semiconducting material, which consists almost exclusively of atoms of an element with four valence electrons, usually Silicon. The transistors consist of an arrangement of regions of the semiconductor that differ in the amount and type of impurity elements they contain. These regions are referred to as either n-type or p-type. In n- (negative) regions, the semiconductor is infused with an element that has an extra valence electron. The extra electrons improve the conductivity of the semiconductor by making the motion of the negatively charged electrons the dominant conduction mechanism. In p-type (positive) regions, the semiconductor is infused with an element with less electrons. This lack of electrons causes the creation of extra holes, a hole being a positively charged electron deficiency.

The transition between a p- and an n-region will normally block the flow of current from the n- to the p-region, but allow current flow from the p- to the n-region. Such a transition is called a diode.

The n- and p-regions can be made in various arrangements to make different types of transistors. The main transistor types are bipolar and field effect transistors.

- Field Effect Transistors (FETs). Although invented first, the first working FET was built later than the bipolar transistor. A particular type of field effect transistor, the Metal-Oxide-Semiconductor Field Effect Transistor (MOSFET) is now the dominant transistor in digital circuits.

- Bipolar transistors. The first transistor type to be made, it was discovered in 1948 in the attempt to build a FET. This work earned William Bradford Shackle, John Bardeen, and Walter Houser Brattain the 1956 Nobel Prize in Physics. Bipolar transistors are the predominant transistors in analog circuits.

This discussion will only deal with the field effect transistor (FET), because it is easier to understand (which is probably why it was invented earlier). In a FET, two regions of the same type are separated by a region of the other type. When the like regions are n-type, this is called an n-channel FET; when the like regions are p-type, this is called a p-channel FET. These two arrangements are illustrated in *Figure 3-6: PNP and NPN Transistors.*

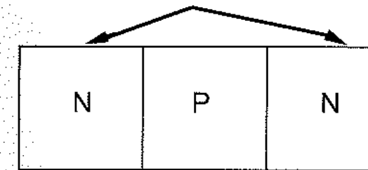

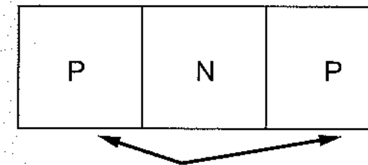

Figure 3-6: PNP and NPN Transistors. p- and n-type regions arranged into p- and n-channel field effect transistors.

If two electrodes are attached to two regions of the same type, and a voltage is applied, this arrangement will not allow current to flow between the two regions because either one of the diodes will block the current flow. However, this situation can be changed by applying an electrical field (hence the term "field effect") to the center region using a third electrode that is electrically isolated from the semiconductor. This electrode is called the gate.

The gate structure can be formed using a metal electrode on top of an insulating oxide layer on top of the semiconductor, giving rise to the term MOS (Metal-Oxide-Semiconductor). When a positive voltage is applied to the gate of an n-channel transistor, additional electrons move to the surface of the p-region. These electrons then form a conductive channel between the two n-regions (hence the name n-channel). Most digital ICs (microprocessors, memory chips) use a technology known as CMOS (Combined MOS) that uses both n- and p-channel MOS transistors.

3.1.5: Integrated circuit production

The production process of integrated circuit involves many steps, which can be grouped into three main steps:

1. Define the structure of the circuit's various components
2. Deposit the material of which the component consists
3. Remove the spurious material.

The structure of an integrated circuit is defined using photolithographic processes. First, a layer of light-sensitive resin is deposited on the wafer. Next, the resin is exposed to a light-dark pattern by projecting a "mask" onto the resin. Finally, depending on the process, either the exposed or non-exposed areas of the resin are removed, and the areas that will not be processed are protected by the remaining resin.

The production process begins with a Silicon disc called a wafer. The wafer is already lightly infused with either n-type or p-type impurities.

After some intermediary steps, the impurities are infused into the wafer in a process called doping. Photolithography processes are again used to define which part of the wafer will be doped. If the original Silicon was slightly doped with n-type material, a p-type region must be made (see *Figure 3-6: PNP and NPN Transistors* (page 29)).

Creation of a p-type region can be accomplished by bombarding the desired area with high energy p-type atoms, which become embedded just beneath the surface. When the Silicon is heated to a very high temperature, the p-type atoms

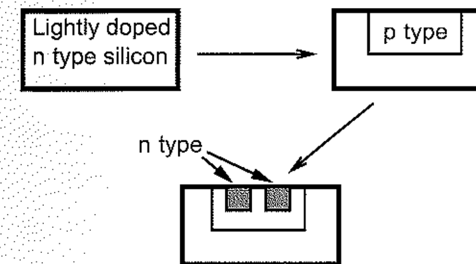

Figure 3-7: Doping Process

will diffuse further down into the Silicon. By controlling the temperature and exposure time, manufacturers can set the depth of the p-type region.

This p-type region is the site of one transistor, which is finally created by adding two small n-type regions. The n-type regions are created with the same method used to create the p-type region. *Figure 3-7: Doping Process* (page 31) shows the steps for implanting the p- and n-type regions into the Silicon wafer, indicating the active area(s) at each stage of the process.

To construct the gate, first the whole piece of Silicon is covered in a thin layer of insulating gate oxide and then covered with a thicker layer of conductive, highly doped polycrystalline Silicon (polysilicon), which behaves like a metal (strictly speaking, the term Metal-Oxide-Semiconductor is not correct for currently produced MOS-FETs).

Next, to ensure that only the gate regions are left covered with polysilicon, the photolithography process is used again. The areas of the oxide and polysilicon that are left exposed can then be removed with suitable chemicals. *Figure 3-8: MOS Transistor* shows the transistor after the unwanted polysilicon has been removed.

Finally, the source and drain are coated with metal for the wiring process, which is accomplished using photolithography. Usually several layers of metal and insulator must be used to make a functional IC.

The benefits of reducing the dimensions of a transistor are clear: the smaller the transistor, the less space required to run a device. The higher the density of transistors on a single chip, the greater the processing power. Decreasing the dimensions is not straightforward, however, and requires intensive research into

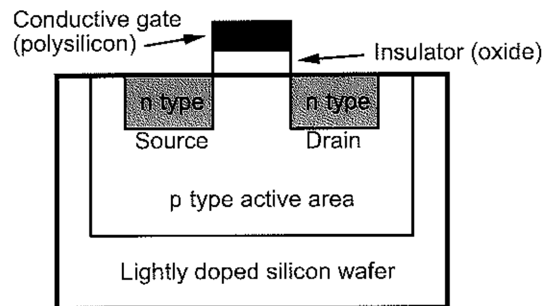

Figure 3-8: MOS Transistor. Cross section of an n-p-n MOS transistor after the gate has been added

all stages of the production process: the production of the semiconducting wafer, the light sensitive resins, the process of the optical projection of the masks, the doping process, the materials and methods used in the production of the insulating oxide layers, and the production of the metal connections.

3.2: Sample Maintenance

CAUTION

- Cleaning the sample is always accompanied by the risk of permanently damaging it.
- To reduce the risk of damaging the sample, it is best to reduce the need for cleaning it by always storing it in its container when not in use.
- Only clean the sample when it has become too dirty to allow good measurements.
- Clean the sample using only highly pure solvents, which prevents the deposition of residues.

To remove any large dust that may have accumulated on its surface, leave the chip and the sample disk in an ultrasonic bath as follows:

1. 10 minutes in distilled water.
   Sonicating the sample in water first removes salts that would not be removed by the subsequent alcohol washing steps.
2. 10 minutes in ethanol.
   Removes finer dirt.
3. 10 minutes in propanol.
   Removes even finer dirt. Using the propanol in the last washing step also results in a cleaner sample after solvent evaporation; it leaves fewer 'spots'.

To ensure that the sample dries as cleanly as possible, remove excess propanol with a clean paper tissue before allowing the sample to air-dry.

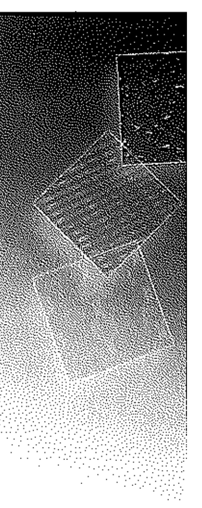

CHAPTER 4:

CD Stamper

Chapter 4: CD Stamper

This sample represents two application areas: Data storage and optical devices. The data storage industry uses the AFM for quality control in the production of various parts of hard disk drives and the masters used for producing CDs and DVDs. Two key capabilities make the AFM the tool of choice with hard disk drives: high resolution z-height measurements and high resolution magnetic field images (using Magnetic Force Microscopy).

In the field of optical data storage and other optical devices (holograms, interference grids), optical surface characterisation tools can not be used because size of the structures is comparable to the wavelength of the light. This makes the AFM the most cost effective tool for surface topography measurement.

The size of CD and DVD structures must be very well-defined, and this requirement is well served by the measurement evaluation tools in AFM software, which is demonstrated in this chapter.

4.1: Measurement

The CD stamper sample contains a piece of the master copy of a CD. This is the original that creates the imprint in the pressed CD that you listen to. A CD has small indentations, called pits, whereas the stamper has bumps in the corresponding places.

4.1.1: Image Acquisition

1. Set a large scan range, approximately 50 µm.

   At this size, you can see many bumps, and it is even possible to make out the curvature of the rows (tracks). Each bump is approximately 200 nm high.

2. Practice zooming in on individual bumps.

   This sample is good for practicing zooming in on individual surface features, as bumps are visible at a variety of scan sizes.

3. Take an image of well-ordered bumps at least 5 or 6 tracks wide.

   Try to get an image similar to *Figure 4-1: 20-µm Image of CD Stamper*, which is suitable for measuring the track distance.

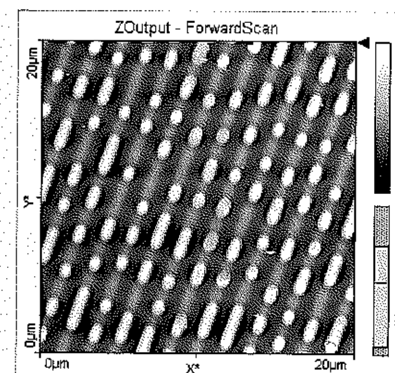

Figure 4-1: 20-µm Image of CD Stamper. Note that the curvature of the tracks is not discernible at this scan range.

4.1.2: Image Analysis

There are two different methods for measuring the track distance. The Measure Length tool measures a cross section, as shown in *Figure 4-2: Track Distance with Length Tool* (page 37), and gives a measurement of 1.63 µm.

The Measure Distance tool, shown in *Figure 4-3: Track Distance with Distance Tool* (page 38), measures the perpendicular distance between two parallel lines. It gives a measurement of 1.598 µm, basically identical to the nominal distance of 1.6 µm.

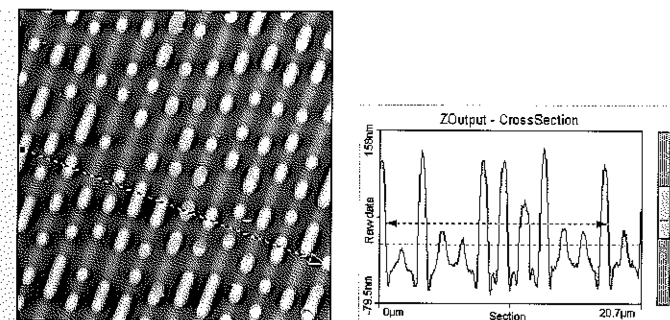

Figure 4-2: Track Distance with Length Tool. Using the Measure Length tool.

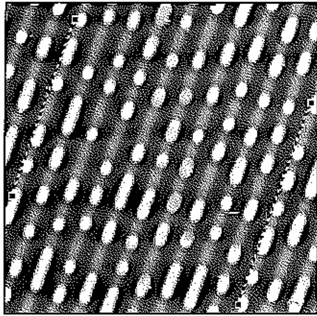

Figure 4-3: Track Distance with Distance Tool. Using the Measure Distance tool.

You can also measure the length of individual bumps in the image. The shortest possible bumps in a CD stamper are approximately 0.8 µm long, while the longest possible bumps are close to 3 µm long.

Figure 4-4: Bump length (page 38) shows a section of the CD stamper along one track (image taken with 20-µm scan range). The length of one of the bumps was measured using the Measure Length tool on a cross section.

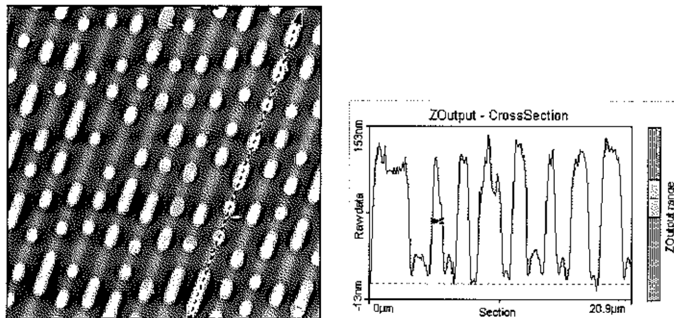

Figure 4-4: Bump length. Using the Measure Length tool in the track direction.

4.2: Optical Data Storage

CDs continue to be the most common optical storage devices. The original music stored on a CD is an analog wave, and the CD stores a digital version of the analog music. This is accomplished by measuring the intensity of the wave at regular intervals and categorizing these measurements into discrete intensity

values. The greater the frequency of the intervals, the closer the approximation of the original wave. The rate at which these measurements are taken is called the sampling rate. A CD uses a sampling rate of approximately 44,000 samples per second, so a CD can store just over 780 million bytes of digital music closely approximating the original analog signal.

4.2.1: Manufacturing

The actual CD stamper is created through a process involving photolithography. An original CD stamper is made on a piece of glass which is polished to ensure flatness and then covered with photoresist. The CD is then exposed to UV light through a mask which has clear parts where the CD will have pits and opaque parts everywhere else. When the CD is then placed in developer solution, only the sections of the photoresist that have been exposed to the radiation will dissolve. Next, the CD master is sputtered with a very thin layer of metal (usually silver). Then it is played to make sure that the process was successful. Finally, the master is covered with a thicker layer of metal. This negative CD is the CD stamper represented by the sample in this kit.

The CD manufacturer uses the stamper to press the shape made by the bumps of the stamper into a piece of polycarbonate plastic. The indented side of the plastic is then sputtered with aluminum and finally covered by a protective layer of acrylic. When a CD player reads the CD, it focuses a laser light beam through the clear polycarbonate plastic layer and onto the aluminum. *Figure 4-5: CD Cross Section* (page 40) illustrates the order in which these layers appear. The laser beam reflects off the aluminum and hits a detector, which simply reads the difference between 1s (the edges of the bumps) and 0s, thus decoding the stored information.

4.2.2: Data Encoding

What is more complicated is the way the CD stores the information in a manner that reduces the chances of errors. This method, called EFM (eight to fourteen modulation) involves converting the original 8 bit data to 14 bit. Adding the extra bits guarantees that there are always between 2 and 10 0s in a row, and never consecutive 1s.

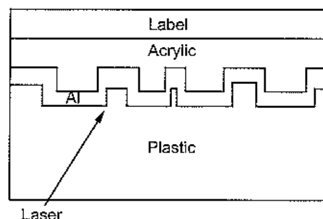

Figure 4-5: CD Cross Section. To read the CD, a laser is focused on the aluminum through the thick plastic layer below the label and aluminum sputter.

Furthermore, CDs use a process called interleaving, whereby information is not stored or retrieved sequentially. The bumps and pits in one track do not make up one long chain of information, but rather scrambled information that the CD reader puts back together. This way, there will never be consecutive numbers, one ending with a 1 and the other beginning with a 1. This process also ensures that if a part of the CD is damaged, there will not be entire sections of a song missing, but rather only split seconds from several songs. Since there are always between 2 and 10 0s together, a CD has between 3 and 11 spaces between 1s, and these 9 lengths are represented by different bump lengths on the CD stamper.

In an image of a large scan range, attempt to locate the smallest bump, and see how many of the 9 lengths you can find in the image. They should approximately correspond to 4/3, 5/3, 6/3, 7/3,..., 11/3 the length of the smallest bump.

Within this information is encoded data that tells the CD player where to read so that you hear the information in the correct order. CDs also use parity check bits, which count the total number of 1s in a string of characters. If the number is even, the check bit would be a 0; if odd, it would be 1. Having many check bits increases the chances of detecting errors in reading the signal.

The final step in being able to hear the encrypted music is the CD player reading the CD. The laser beam that reads the CD has to stay focused on the track at all times, so the beam and the detector slowly move along the CD in the radial direction as the information is read. At the same time as it moves outward, though, the speed of the bumps increases, since the speed is equal to the radius times the rotational speed. As the reader moves outward, the CD player has to

slowly decrease its speed to make sure that the information is always read at the same rate.

4.3: Sample Maintenance

CAUTION

- Cleaning the sample is always accompanied by the risk of permanently damaging it.
- To reduce the risk of damaging the sample, it is best to reduce the need for cleaning it by always storing it in its container when not in use.
- Only clean the sample when it has become too dirty to allow good measurements.
- Clean the sample using only highly pure solvents, which prevents the deposition of residues.

To remove any large dust that may have accumulated on the surface, leave the chip and the sample disk in an ultrasonic bath as follows:

1. 10 minutes in distilled water.
   Sonicating first in water removes any salt, which would not be removed by the alcohol.
2. 10 minutes in ethanol.
   Removes finer dirt.
3. 10 minutes in propanol.
   Removes even finer dirt. Using the propanol last also leaves the sample cleaner, as it evaporates, leaving fewer spots.
4. To ensure that the sample dries as cleanly as possible, dab it off with a clean paper tissue to remove excess propanol when removing it from the propanol.

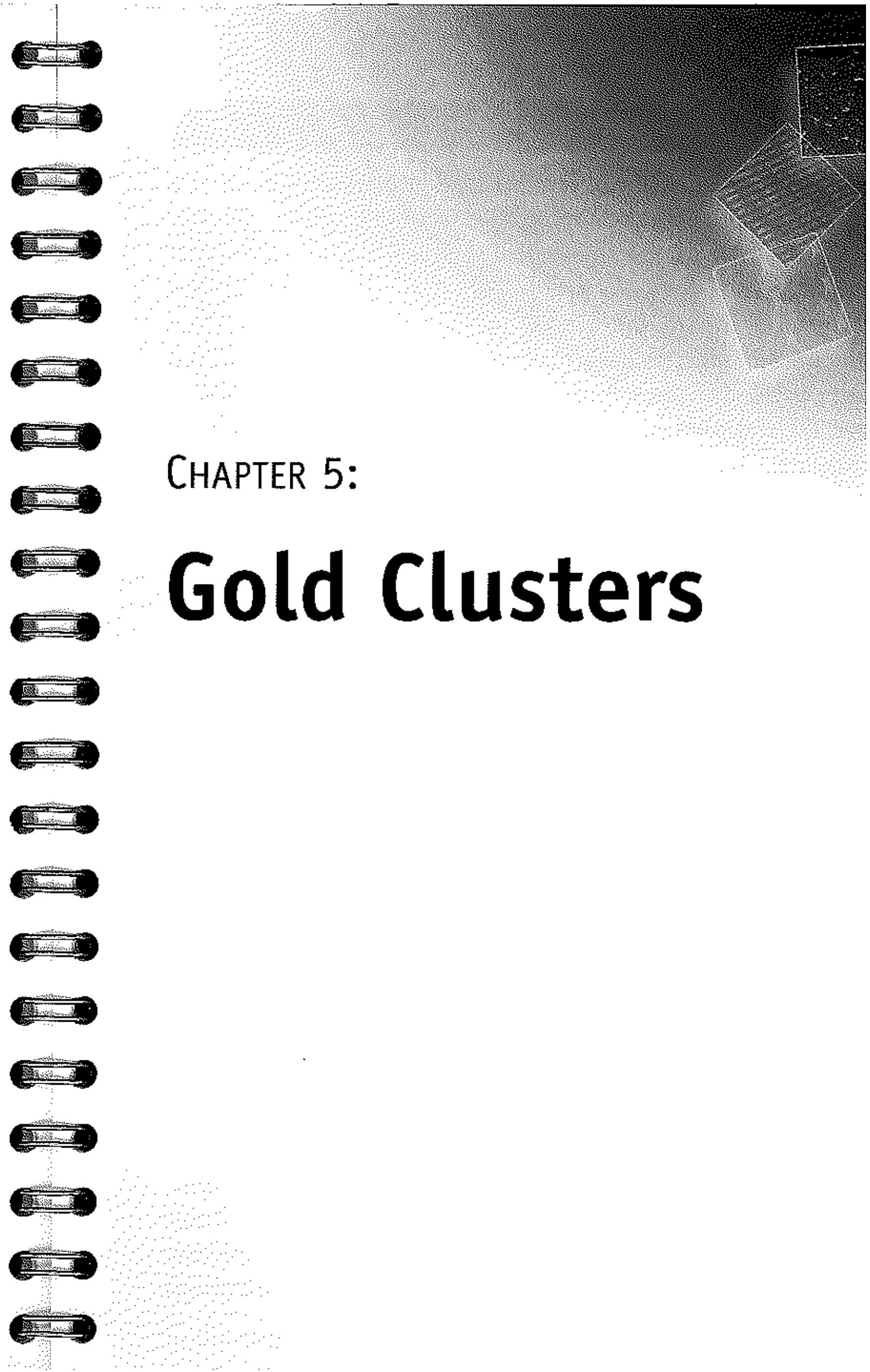

CHAPTER 5:

Gold Clusters

Chapter 5: Gold Clusters

The gold clusters sample consists of a thin layer of gold clusters on a piece of a silicon wafer. This sample represents the application area of thin film coatings. Although the techniques used for producing coatings are in many respects similar to the techniques used for chip production, they differ in both the surface area that is coated and in the greater variety of materials used for coatings. Moreover, the thin film coating processes are meant to change the function of the entire surface of the sample as opposed to producing discrete structures. Therefore, AFM applications concentrate on characterizing statistical properties of these coatings, rather than the size of specific structures.

The most commonly used statistical property of a surface is roughness, of which there are many different parameters. This chapter shows how AFM measurements are used to determine the surface root-mean-squared roughness parameter (Sq) of the gold cluster sample.

5.1: Measurement

5.1.1: Image Acquisition

The maximum height value attained in the topography of the gold clusters sample is close to 10 nm, not taking into account any dirt that may appear on the surface. The image in *Figure 5-1: Image of the Gold Clusters Sample* (page 45) appears to be free of any dirt. Starting with a large scan range (1.5 µm) allows you to identify any potential dirt so you can locate a smaller area free of dirt and zoom in on it.

This sample is quite smooth, i.e., has a very low roughness. Therefore, the measurements are very sensitive to disturbances, meaning there is more noise apparent in the height signal. The horizontal lines across the images are noise that is inherent to images taken with any scanning instrument such as an AFM. The noise is not an important factor in height signals above 30 or 40 nm, since the signal-to-noise ratio is very high. In very flat samples, however, the lower ratio results in an image with lower resolution. To reduce the effects of the noise, cover the microscope with a padded cover and/or keep it on a vibration isolated table.

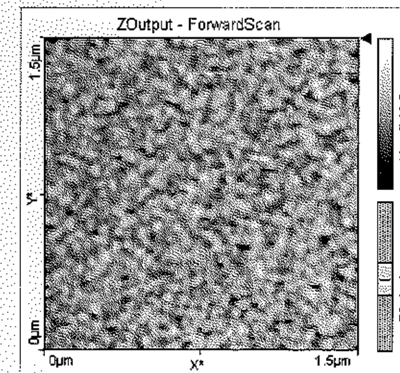

Figure 5-1: Image of the Gold Clusters Sample

In a scan range of about 10 µm, many clusters are present but not always apparent. The clusters vary in size, but they are typically round with a diameter of approximately 100 nm. In a scan range of 10 µm, there will be close to 100 clusters across the image, which makes it difficult to resolve individual structures. *Figure 5-1: Image of the Gold Clusters Sample* shows a scan range of 1.5 µm, and even in this range it is difficult to resolve individual clusters with much certainty.

5.1.2: Image Analysis

The gold cluster sample is useful for introducing the concept of roughness. Roughness is one type of deviation of the sample surface from an ideal surface. For plane surfaces, the only other type of deviation is called waviness. The opposite of roughness is smoothness; the opposite of waviness is flatness. The separation between roughness and waviness is determined by the lateral scale: long variations are wavy, short variations are rough. The distinction between roughness and waviness is made because roughness generally has a different effect on the function of a device than waviness. For example in optical devices, waviness causes optical aberrations; roughness causes light dispersion and absorption.

In the easyScan software, the surface roughness is calculated as follows:

Before doing any evaluation on the data shown in chart, the software processes the height data according data filter that was set View Panel, or chart Bar, depending on the software that you are using. Before calculating roughness, subtract the average slope of the data by selecting the Line fit/Plane fit data filter.

In *Figure 5-1: Image of the Gold Clusters Sample* (page 45) the number of points is expressed as the number of data samples taken: 256. This means that the microscope will record 256 lines of data (in the y-direction), with each line consisting of 256 equally spaced data points (in the x-direction).

The Root-Mean-Square (RMS) roughness, Sq, is defined to be the sum of the absolute value of the difference of the height at each point and the mean height. It is therefore a measure of how different the height of the sample is from its average height, which is the value calculated by

$$S_q = \sqrt{\frac{1}{n^2}\sum_{i}^{n}\sum_{j}^{n} z_{ij}^2}$$

Since height is measured in nm, the difference will also be in nm. The square of the difference will be in nm^2, and Sq will be measured in nm. For a sample with perfectly uniform height, the height of each point will be equal to the mean height. The difference between the mean and the height at each point will be zero, so the RMS roughness will also be zero.

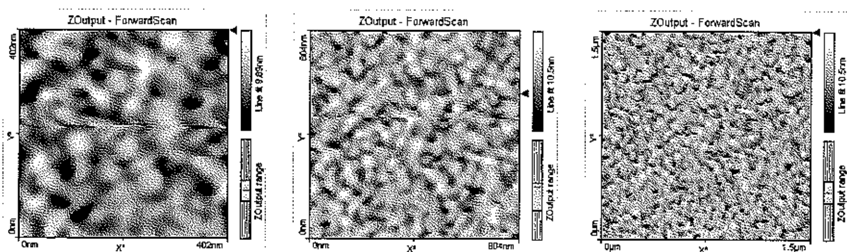

Figure 5-2: Scan Speed and Roughness. Gold clusters sample scanned at 400 nm, 800 nm, and 1500 nm, at the same scan rate (time/scan line).

In *Figure 5-2: Scan Speed and Roughness* shows scans of the gold clusters sample taken at three different scan ranges, all centerd on the same point, and scanned

at the same rate. Roughness analysis was performed on each. The roughness analysis on the smallest scan region (400 nm) image yielded a Sq of 1.6 nm. The next larger scan region (800 nm) had a slightly smaller Sq of 1.58 nm, and the largest region (1500 nm) yields a still smaller value of 1.3 nm.

One possible explanation for this change in roughness is that the measurement speed is too high at the larger scan sizes, so the tip does not follow the surface as accurately. As the scan sizes increase, the scan rate (lines of data recorded per second) remains the same, so the probe tip encounters variances in the surface topography at a faster rate. This makes it harder for the feedback loop to follow the topography. Investigate this by measuring the same area with different scan rates.

5.2: Fabrication of the Gold Clusters

The gold clusters sample consists of a thin layer of gold clusters on a piece of a silicon wafer. To help the gold stick to the surface, a 5-nm layer of titanium was applied to the surface before adding the gold. The gold layer is 200 nm thick. As the gold atoms were deposited on the titanium, they joined into clusters on the surface.

To prepare the sample, small pieces of the silicon wafer were cut to fit onto the sample disc. The pieces were then cleaned in a sonic bath for a few minutes each in water, acetone, ethanol, and finally propanol. The cleaning ensures that the silicon has no pieces of dirt on its surface, which would result in an uneven coating of titanium and gold.

Both the titanium and the gold were applied to the silicon with the use of a sputtering machine. Samples of titanium and gold are at the bottom of the chamber, with the silicon samples at the top, as shown in *Figure 5-3: Sputtering machine* (page 48). The titanium and gold are bombarded with high energy argon ions to release metallic atoms.

The atoms that are released are actually ions, meaning they have electric charge. A strong magnetic field is applied in the chamber, and the charged titanium and gold atoms are directed upwards in the field onto the silicon. By controlling the pressure in the chamber and the exposure time of the silicon, the exact thickness of titanium and gold layers can be controlled.

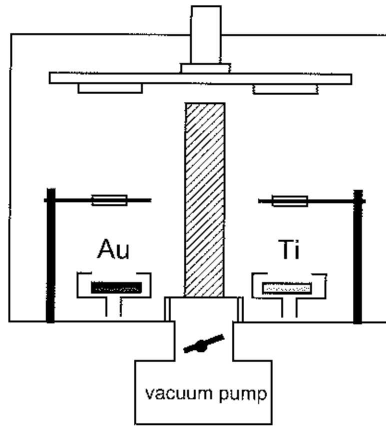

Figure 5-3: Sputtering machine. The vacuum pump controls the pressure inside the chamber. The boxes directly above the gold and titanium are sensors that measure the rate at which the metals are applied to the silicon above (the rectangles above the sensors). The lines that run through the sensors are the shutters that open or close depending on which metal is being applied to the silicon.

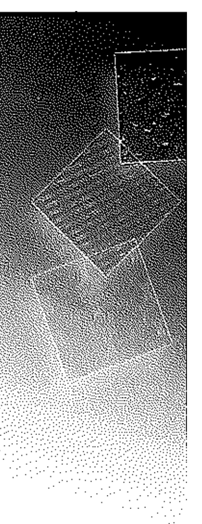

CHAPTER 6: Nanotubes

CHAPTER 6: Nanotubes

The carbon nanotube sample represents the group of materials with macromolecules that are used for molecular nanotechnology. Other well-known examples are self-assembled particles, DNA, and nanotubes made of other materials.

AFMs can be used to characterize and manipulate such molecules. The well-defined structure of nanotubes makes them ideal for demonstrating the influence the structure of the end of the AFM tip has on the measured image. While manipulation is not demonstrated here, that does not mean it is impossible to do.

6.1: Measurement

The carbon nanotube sample consists of a piece of silicon wafer on which carbon nanotubes are deposited. Nanotubes are less than 10 nm in diameter and can reach lengths of several 100 micrometers.

6.1.1: Image Acquisition

With this sample, the tip is likely to be damaged, if the scan parameters are not well optimized. Therefore, if you start with a relatively large range (~ 15 µm) and successively zoom in on an area of interest, it may not be possible to measure the nanotubes at high resolution. *Figure 6-1: Nanotube Images* (page 51) shows images of nanotubes taken at optimal and less than optimal settings.

1. Set a small scan range (2 µm or less).
2. Take a scan.
3. Optimize scanning parameters
4. Zoom out by taking a scan at a relatively large scan range (~15 µm).
5. Identify an area of interest.
6. Zoom back in.

Figure 6-2: Optimizing the Set Point illustrates an optimization sequence. At first, the set point is too high (10nN), so the nanotube gets pushed around. This makes it appear streaky and not as wide as it should be. With the Set Point

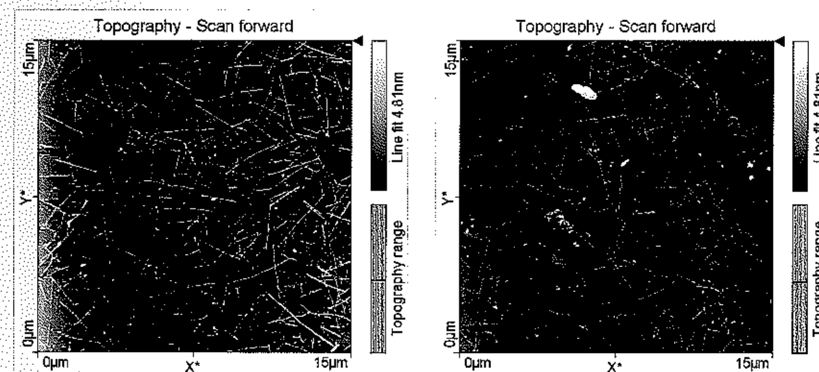

Figure 6-1: Nanotube Images. (Left) Blunt tip and set point too high (19 nN). (Right) Sharp tip and better set point (2nN).

lowered, the nanotube is imaged more stably. Note that the dirt that was pushed to the side in the first scan is visible on the side of the second scan.

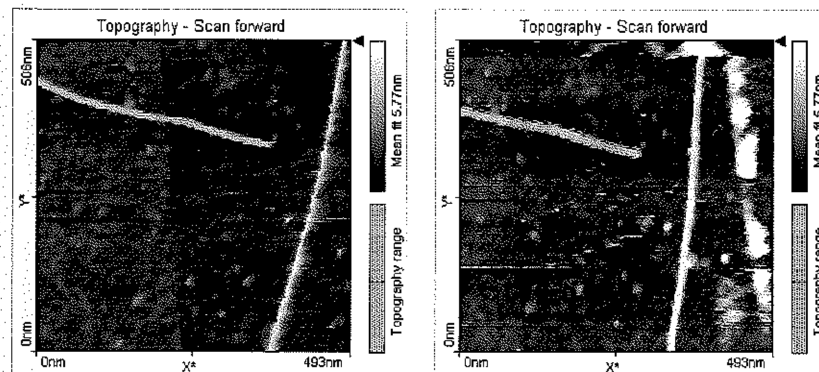

Figure 6-2: Optimizing the Set Point. (Left) Force set point (10 nN) is too high. (Right) Lower force set point (2 nN). Note the dirt moved around by the previous measurement with excessive force set point.

6.1.2: Image Analysis

Length

Use the length tool to measure the length of various nanotubes. For best results, measure the straighter nanotubes, as the curved or bent ones may be difficult to

measure. Compare the lengths of the longer nanotubes to the shortest ones, and note the wide variations.

Height and Width

Use the section tool to measure the height and the width of a nanotube. First, use the line section tool to draw a line perpendicular to the axis of the nanotube to be measured. Then measure the nanotube height using the distance tool, and measure the width using the length tool. *Figure 6-3: Nanotube Cross Section Measurements* (page 52) shows how tip sharpness affects the measurements.

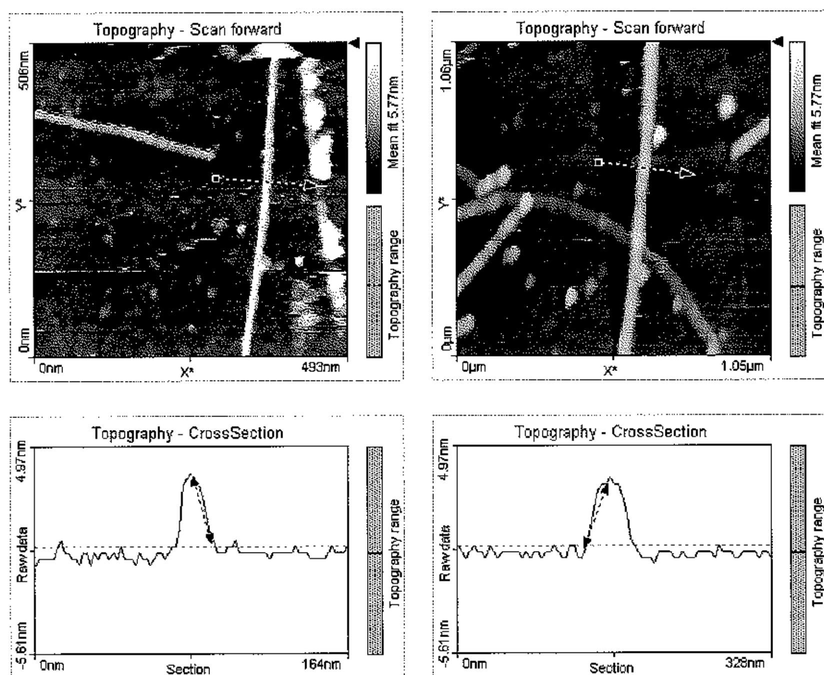

Figure 6-3: Nanotube Cross Section Measurements. (Left) With sharp tip, height is 3.7 nm, width is 20 nm. (Right) With blunt tip, height is 3.6 nm, width is 47 nm.

Tip Geometry

In theory, nanotubes are cylindrical. The above measurements indicate that the vertical distance between the top of one nanotube and the silicon substrate is

around 3.6 nm, which is the nominal diameter. The width measurements, however, clearly do not represent a cylinder with this diameter.

The reason for this discrepancy is that the horizontal measurements are limited by the shape of the end of the tip. A simple model of the end of the tip is a sphere. When a sphere scans over a cylinder that is smaller than the sphere radius, the measured topography will be a cut-off cylinder with a radius equal to the sum of the radii of the tip and the cylinder. The top of the cut-off cylinder will have the same height as the actual cylinder (i.e. the nanotube.), as illustrated in *Figure 6-4: Nanotube–Tip Geometry.*

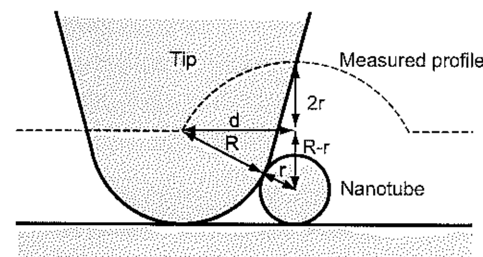

Figure 6-4: Nanotube–Tip Geometry. The larger circle represents the end of the tip, where it is approximately spherical. The smaller circle is the cross sectional view of a nanotube. By setting up a right triangle whose hypotenuse is the line joining the centers of the two circle, it is possible to calculate the tip radius.

Notice that the shape of the tip does not permit it to touch the silicon surface at the edge of the nanotube. Since the tip is approximately spherical, there is a significant area of the silicon surface on either side of the nanotube that it cannot touch. At the point where it does touch the silicon surface, a right triangle can be constructed to approximate the actual tip radius, as shown in *Figure 6-4: Nanotube–Tip Geometry.*

One leg of the triangle has length d, which is the horizontal distance measured from the highest point on the nanotube to the point where the tip touches the silicon. The other leg is R-r, which is the radius of the tip minus the radius of the nanotube. The hypotenuse is the sum of the two radii. Using the Pythagorean relationship, we find that:

$$(R-r)^2 + d^2 = (R+r)^2,$$

$$R^2 - 2rR + r^2 + d^2 = R + 2rR + r^2,$$

$$d^2 = 4rR, \text{ and}$$

$$R = \frac{d^2}{4r}$$

Entering the values determined from the analysis in *Figure 6-3: Nanotube Cross Section Measurements* (page 52) (d = 10 nm and 23.5 nm, and r = 1.8 nm) gives a tip radius R of approximately 14 nm for the sharp tip. This is reasonable, considering that the nominal tip radius given by the manufacturer is 10 nm. For the blunt tip (d = 10 nm and 23.5 nm, and r = 1.8 nm), the tip radius becomes 77 nm.

6.2: Carbon Nanotubes

A carbon nanotube is, as the name suggests, a tiny cylinder composed of carbon atoms. More specifically, it is a lattice of graphitic carbon rolled into a tube. *Figure 6-5: Nanotube Molecular Structure* (page 55) shows an example of the molecular structure of a carbon nanotube. The ends of the tube in *Figure 6-5: Nanotube Molecular Structure* (page 55) are not capped, but it is possible to seal a nanotube at both ends with a fullerene. A fullerene is similar to a nanotube in molecular structure, but it is spherical rather than cylindrical.

The bonds that hold nanotubes together are entirely sp2 bonds, as in graphite. These bonds are stronger than the chemical bonds of diamonds, making nanotubes very durable. Nanotubes naturally align themselves into bundles held together by Van der Waals forces.

Japanese physicist Sumio Iijima discovered the hollow, cylindrical nanotubes while studying fullerene synthesis in 1991. Today, nanotubes are used in a range of applications that is remarkable considering their short history.

A nanotube may or may not conduct electricity, depending on its structure. This opens the possibility of very tiny electrical circuit elements, particularly transistors (see the description in the Chip Structure chapter). Nanotubes have

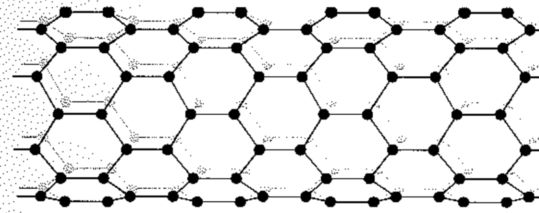

Figure 6-5: Nanotube Molecular Structure

also been shown to conduct heat very effectively, a property that could be applied to the cooling of tiny mechanical elements. It has also been shown that by removing the cap at one end of a nanotube, it can be used as a nano-test-tube.

Under the proper conditions, nanotubes can be made sufficiently long to serve as carbon fibres. Researchers have found that newly synthesized nanotubes exhibit strong absorption of outside molecules, and this may have direct applications in medicine. A company called Babolat uses nanotubes in their tennis rackets to keep them stiffer, and controlled electron emission from nanotubes have been used in television-like displays. Building nanotubes will become simpler and more cost efficient as research into their production continues, likely leading to an even greater prevalence in their use and a further expansion in the variety their applications.

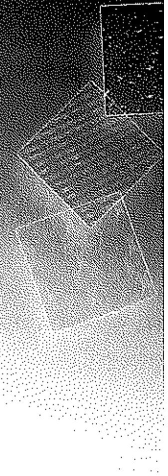

CHAPTER 7:

Glass Beads

Chapter 7: Glass Beads

The glass beads sample is a piece of glass covered with a thin layer of very small colloidal silica (i.e., glass) particles. The beads will group in clusters, some of which exhibit crystalline structures. Colloidal particles are often used to make small scale regular structures, such as calibration patterns, hard disk-recording media, and photonic crystals. AFM can be used to characterize defects in such structures, but here the structure is used to characterize the 3D-shape of the AFM tip, as opposed to the 2D characterization done with nanotubes in the previous chapter.

7.1: Measurements

7.1.1: Sample Preparation

The glass bead sample must be prepared. The kit contains an empty glass slide and a vial of diluted bead solution, which will be used to create the sample. In this case the beads have a diameter of 120 nm (may vary in future). Once the sample is prepared, it can be used for measurements as long as it remains clean.To prepare the sample:

1. Take the following materials from the sample kit:
   - Glass slide
   - Diluted bead solution
   - Ethanol
   - Clean tissue
2. Clean the glass slide and remove any accumulated dirt:
   - A. Drip some ethanol on the slide.
   - B. Wipe the ethanol off with the clean tissue.
3. Place the vial with the bead solution in a beaker partly filled with water.
4. Place the beaker in an ultrasonic bath for approximately 20 minutes.
   This process will break up any groupings of beads in the solution. The beads will form aggregates over time due to simple attractive interactions between

   them (such as Van der Waals forces), but the goal is to have individual beads come together on the glass slide and eventually form crystalline structures.
5. Use an eyedropper to place a drop of bead solution onto the cleaned glass slide.
6. Try to form the largest drop possible without spilling over the sides of the glass.
7. Dry the sample under ambient conditions.
   This may take several hours.
8. Fix the beads by baking:
   - A. Place the sample disc in an oven at 250° for 2–3 hours.
   - B. Allow the sample to cool completely before imaging

7.1.2: Image Acquisition

Approaching the Sample

This sample is one of the more difficult to approach, as it is non-metallic, and not very reflective. If you can see the cantilever's shadow or reflection, you can use it to judge the distance. If you find it difficult to recognise the cantilever's reflection, then slightly move the sample holder: the structures on the sample will move, but the reflection will stay in the same place.

If you cannot see the cantilever's reflection, perform a very slow coarse approach while judging the distance on the focal plane of the side view as follows:

- When the tip is on the sample, the focal plane crosses the sample at the tip position.
- When the tip is further away, the focal plane crosses the sample more behind the cantilever.

Scanning

1. Start with a low force set point for best results.

   Applying too much force may move some of the beads around and create wide horizontal stripes across the image.

   If you get stripes in your image:

   A. Lift the tip, and then
   B. Bring it back into contact.

   If the tip is simply dirty, you can remove the dirt by:

   A. Retracting the tip
   B. Re-extending it again.

   If there are still stripes in your image, the problem may be that the region where you are scanning does not have perfectly fixed beads. In a region of more ordered beads, the beads will stay in place. Therefore:

   - Move to another region on the sample.

2. Set the scan range to 1 µm.

   Since the beads are approximately 120 nm in diameter, you should be able to see about 10 of them across the image.

   If your image shows islands of beads surrounded by very flat areas:

   - Move to a region of better ordered beads.

In general, the region with the best ordering is close to the center of the spot on the slide. *Figure 7-1: Well Ordered Beads* shows a well-ordered region near the center of the spot.

Identifying the Bead Structure

In a well ordered region, each bead will be surrounded by 6 others. Identify a single bead, and count the beads around it to see if it is surrounded by 6 others. Then check to see if each of these 6 beads is, in turn, surrounded by 6 others.

In *Figure 7-1: Well Ordered Beads*, for example, the top right corner of the image is far better ordered than the top left. Notice also that there are some beads slightly higher up than others; they are not all perfectly coplanar.

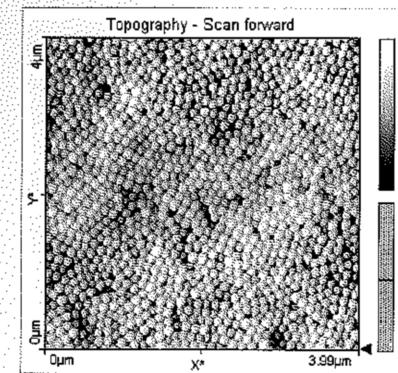

Figure 7-1: Well Ordered Beads. The center part of a spot of bead solution. Some sections have a crystalline structure while others are less ordered.

7.1.3: Image Analysis

Section analysis can be used to determine the distance between desired markers. *Figure 7-2: Bead Section Analysis* (page 62) illustrates how to find the vertical distance from the point from where two beads touch to the top of one of the two beads. Since the beads are approximately spherical, and have a 120 nm diameter, the vertical distance between one peak and the adjacent valley should be half the diameter (60 nm). However, in this section analysis, the vertical distance is only about 15 nm. The discrepancy is due to the fact that scanning is limited by the shape of the tip, which cannot fully extend down between beads.

Figure 7-3: Bead-tip geometry (page 63) illustrates how this occurs with a tip that is approximately spherical at the end. The tip may track some of the height drop between two adjacent beads, but it will not track the full extent of the drop. While this effect is negligible for larger beads, it becomes more significant the smaller the beads are.

The radius of the tip can be calculated from three pieces of information:

1. The radius R of the beads.
2. The radius r of the tip.
3. the height h between the tops of the beads and the lowest point that the tip reaches between them.

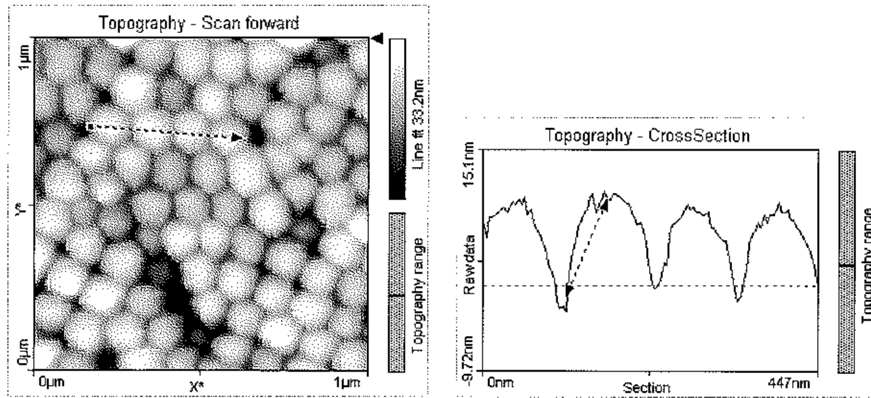

Figure 7-2: Bead Section Analysis. A section analysis of a zoomed in area of the bead sample.

Simple geometry predicts:

$$R^2 + (R + r - h)^2 = (R + r)^2$$

Rearranging that formula provides the following equation to calculate the tip radius:

$$r = \frac{(R - h)^2}{2h}$$

Using h = 15 nm and R = 60 nm, we find that the tip has an approximate radius of 68 nm. The manufacturer specifications for the tip radius is 10 nm, so this is rather large. It is possible that one or more beads are clinging to the end of the tip, causing the aparent increasy in tip radius.

The method outlined above is an easy way to estimate the actual tip radius. Also, we learned that the tip radius influences the image feature size, especially when the two have comparable dimensions.

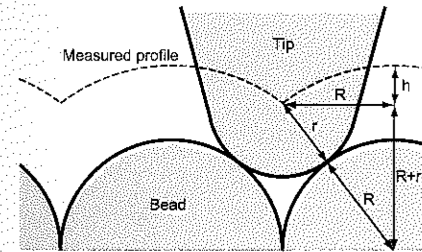

Figure 7-3: Bead-tip geometry. The tip may not fit all the way down between two beads. The geometry of the beads and the tip allow the determination of the tip radius.

7.2: Relevance of the Glass Beads

The glass beads sample demonstrates the small scale interactions of sub-micron bodies. This alone is an interesting use for the beads, but many other uses exist.

Different sized beads have been shown to disrupt different cells. Cell disruption is the process wherein the cell wall growth is disturbed for the purpose of extracting products out of the cells in which they are produced. This disruption can be used, for example, to obtain DNA from within a cell nucleus. Extensive research has been performed, and now sold in different sizes according to their use in specific cells.

Beads have also been very useful in the study of chromatography, the separation of a mixture of substances in a phase separated medium. There is a stationary phase, held in some sort of container, and a moving phase flowing through it. The different substances in a given mixture are drawn to either the stationary or mobile phases based on some property (size, charge, etc.) that they exhibit.

Silica beads coated with a substance similar to that of a cell membrane have been used to simulate cellular interactions. This provides a simple way to reproduce crucial biological phenomena that are not fully understood. In other experiments, researchers have suggested that silica beads coated with gold may kill cancerous cells when exposed to near-infrared light.

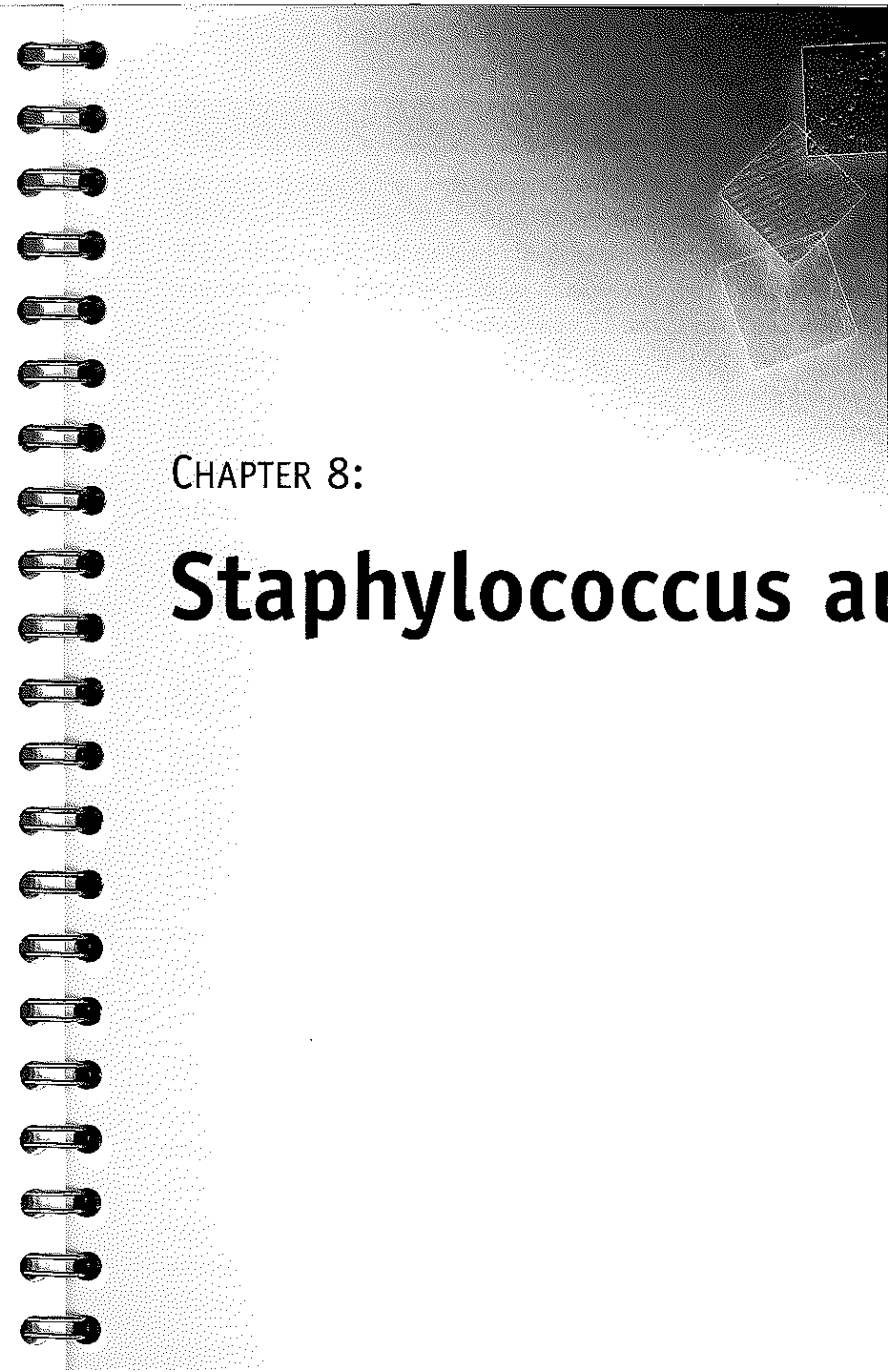

CHAPTER 8:

Staphylococcus a

Chapter 8: Staphylococcus aureus

AFM is used for various biological applications, such as determining the structure of proteins and the binding force between antibodies and antigens and other key-lock pairs. While most of these measurements must be performed in a physiological solution, some samples, such as the Staphylococcus Aureus sample, can be measured under normal AFM scanning conditions.

The staphylococcus (staph) aureus bacteria sample is a glass slide covered with millions of bacteria. The bacteria have been killed and fixed to the slide, so the sample is safe to touch and scan. The name staphylococcus comes from the Greek word staphylos, meaning "bunch of grapes," and the Latin word coccus for the round shape of the individual bacterium. Aureus is a strain of the staphylococcus bacteria, one which is commonly contracted by humans. The round bacteria group together in random clusters, which makes them look like grapes in bunches.

8.1: Measurement

8.1.1: Image Acquisition

The glass slide is only slightly reflective, so it can be difficult to judge the tip–sample distance for the approach. If you can see the cantilever's shadow or reflection, you can use it to judge the distance. You can try to make the reflection more visible by moving the sample holder slightly.

If you cannot see the cantilever's reflection, perform a very slow coarse approach while judging the distance on the focal plane of the side view as follows:

- When the tip is on the sample, the focal plane crosses the sample at the tip position.
- When the tip is further away, the focal plane crosses the sample more behind the cantilever.

The bacteria have been fixed to the glass slide with a burning process. The process leaves a mark where the bacteria have been burned, which makes it possible to locate the parts of the slide that are covered with bacteria.

8.1.2: Image Analysis

The individual bacteria are approximately 0.7 µm in diameter, so it is possible to make out several bacteria in a relatively large scan range. This sample has regions with a very high concentration of bacteria as well as some with lower concentrations and some bare spots. The left image in *Figure 8-1: Staphylococcus Bacteria Images* shows a 20-µm scan region densely packed with bacteria. It should be easy to zoom in on a much smaller scan region where the bacteria are still very concentrated.

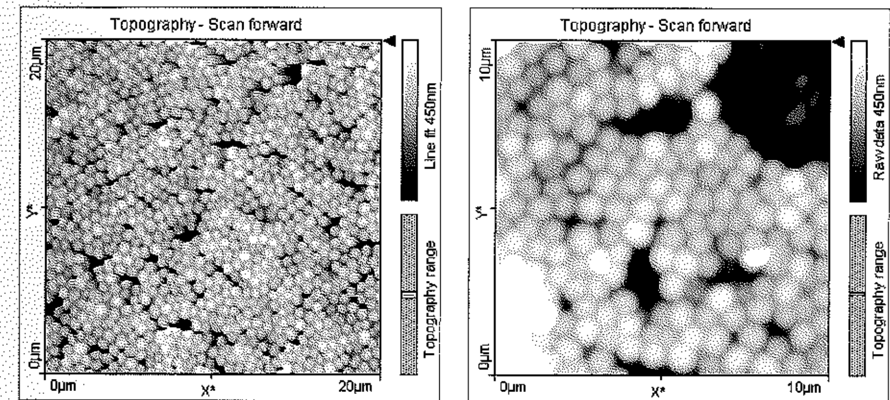

Figure 8-1: Staphylococcus Bacteria Images. (Left) Topography with a scan range of 20 µm. Some regions appear to have almost crystalline structure, while other regions contain unordered gaps. The variations in color brightness of the individual bacteria correspond to the variations in height of the bacteria. (Right) Topography with a scan range of 10 µm. Both images have a height scale of 450 nm.

The image of the 10-µm scan on the right shows a less dense region. In a scan range of this size, and where the bacteria are less dense, it is clear why the bacteria were named after grapes. The round bacteria appear like individual grapes, and clusters like the one in the top right corner appear like bunches of grapes.

The height scale of 450 nm is small considering that the free bacteria are spherical with an approximate diameter of 0.7µm. It is likely that the process which fixes the bacteria to the slide results in flattening them as well.

Figure 8-2: 3D View (page 68) is a parallel perspective projection of the 3D data of the same measurement. The height scale is exaggerated with respect to the X

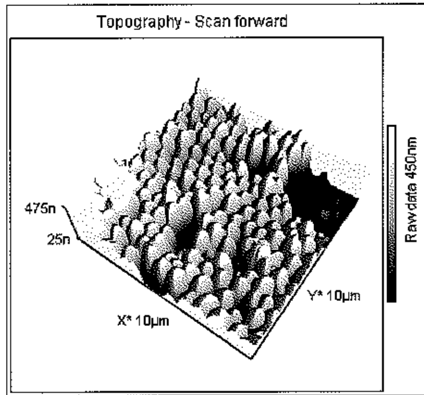

Figure 8-2: 3D View. A parallel perspective projection of the same dataas the 10-µm scan range image in *Figure 8-1: Staphylococcus Bacteria Images* (right image) shows that some bacteria are stacked on top of others.

and Y scale; the bacteria appear to be much higher than they actually are. Each view illustrates a different feature of the sample. The color map image emphasizes the round shape of the bacteria, as well as their random horizontal clustering and bare spots. The color map image provides color contrast, which makes it possible to determine that some bacteria are higher than others through the color scale, but the 3D view directly shows that some bacteria are clearly stacked on top of several others.

Figure 8-3: Zoomed Image (page 69), left, shows the bacteria using a 5-µm scan range. Zooming in on the bacteria highlights the topographical features of the individual bacteria. The fine grains that are visible on the surface of the bacteria in *Figure 8-3: Zoomed Image* (page 69) were not visible in *Figure 8-1: Staphylococcus Bacteria Images* (page 67). This is not because the bacteria in the smaller scan range are different. Rather, zooming in allows smaller details to be captured at higher resolution.

Figure 8-3: Zoomed Image (page 69), right, shows the height difference between consecutively measured points (also called derived data). This image displays the slope of the topography and gives better contrast for finer details. For example, the textured surface of the bacteria is enhanced in the deflection image, as is the shape of the cell walls separating the bacteria.

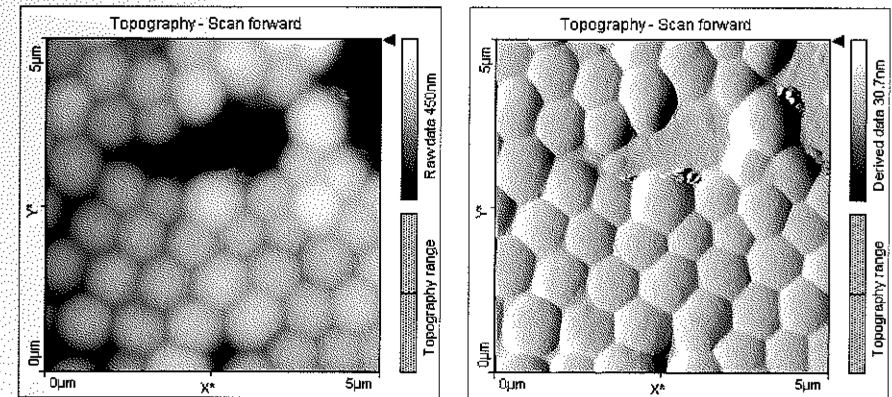

Figure 8-3: Zoomed Image. (Left) Color map chart of raw data. (Right) Color map chart of derived data. The maximum height attained in the image on the left is 450 nm. The height scale for the image on the right is arbitrary, in the sense that it has nothing to do with the height of the bacteria.

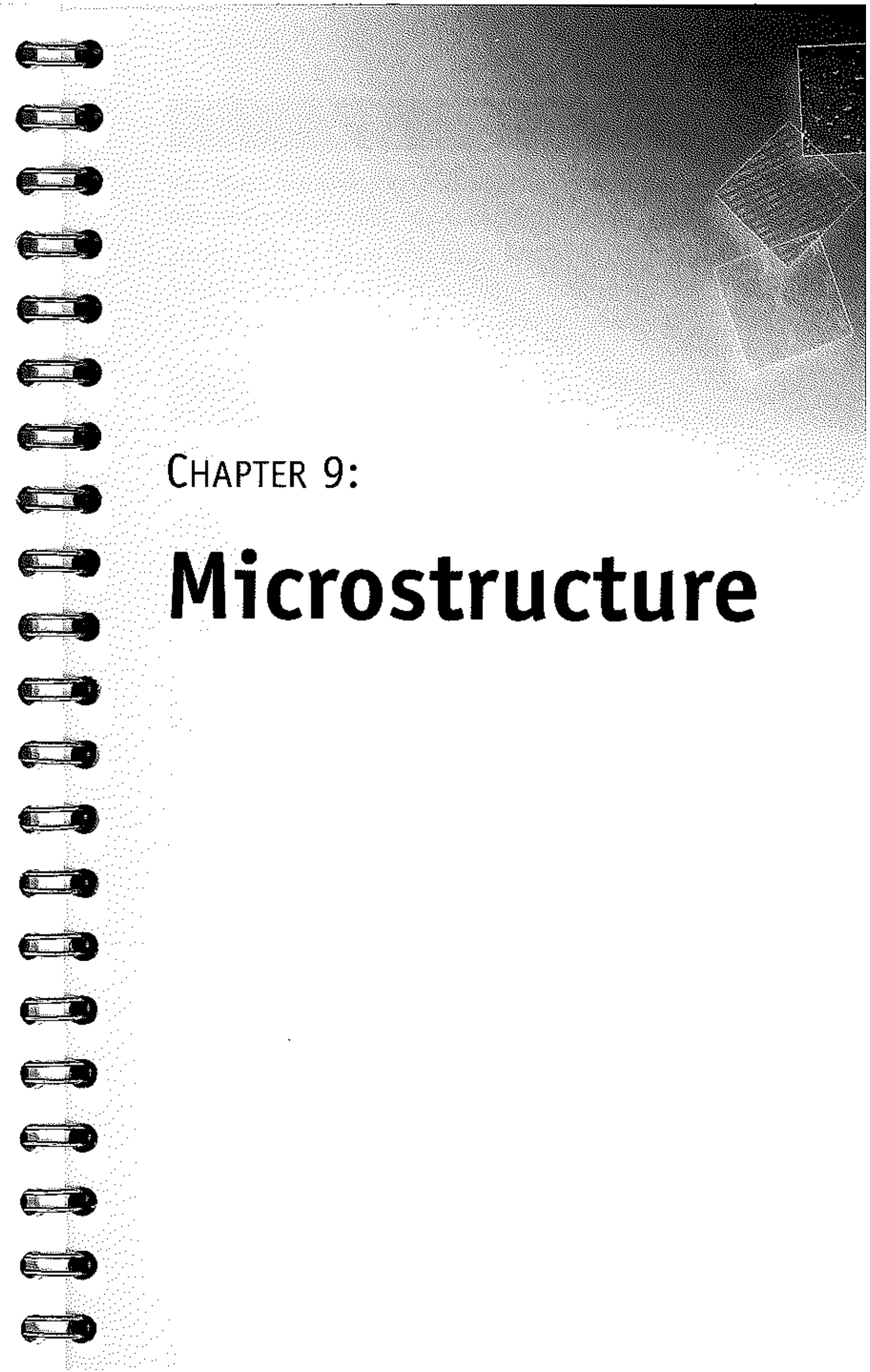

CHAPTER 9:

Microstructure

CHAPTER 9: Microstructure

The microstructure sample consists of a structured silicon dioxide layer on silicon. The structures are regularly distributed squares. Depending on the stock, the sample has square silicon dioxide island or square holes in the silicon dioxide layer. This kind of sample is often used to calibrate the orthogonality of a microscope imaging device.

9.1: Measurement

This sample is in general quite easy to measure and there are not any special settings to be considered. However due to the abrasive characteristics of the oxide layer, the tip quality decreases quite fast compared to usual tip wear. Thanks to the sharp steps, this sample is ideal to learn and train how to optimize the PID feedback settings and vibration amplitude in dynamic mode. The later will be the subject of the analysis section.

9.1.1: Image Acquisition

The general guide how to start a measurement is described in the operating instructions. In this particular case:

1. Find a clean spot on the sample
2. Approach the sample
3. Start the measurement
4. Adjust the slope
   The procedure for adjusting the slope is described in the operating instructions.
5. Adjust PID gains
6. Find the optimum vibration amplitude (see next section)

9.1.2: Image Analysis

Setting the vibration amplitude is crucial for achieving the best possible resolution. In static mode, the main parameter to regulate the image quality are the PID feedback settings and the Set point. In dynamic mode, the setting of the

vibration amplitude additionally plays an important role. In general, the vibration amplitude must correspond to the size of the sample features:

- Low structures require a small amplitude
- High structures require a big amplitude.
- Small structures on top of big structures require a small amplitude and a slow scan speed.

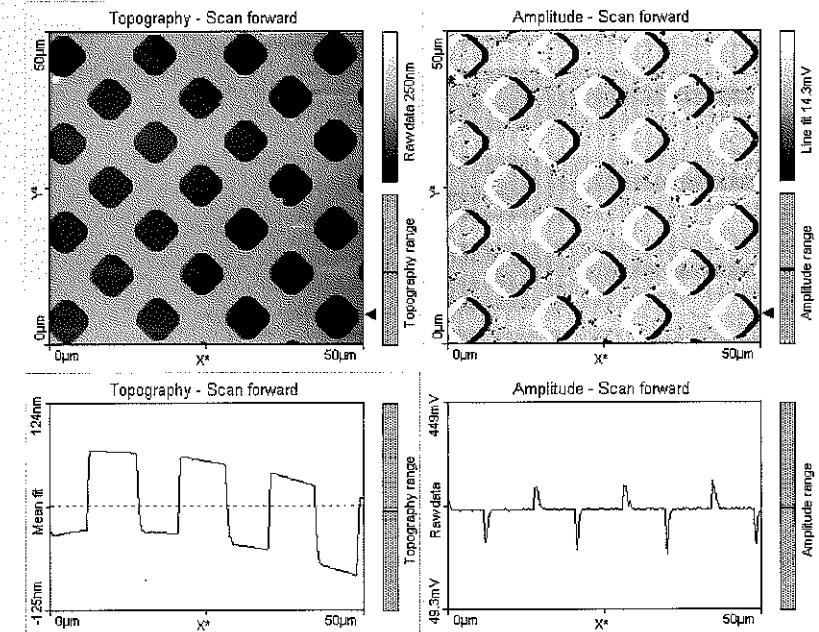

Figure 9-1: Large Amplitude. Topography and amplitude image of the microstructure sample. The line graphs show a cross section of the images above at the position indicated by the arrow. The vibration amplitude was set to 400 mV.

Figure 9-1: Large Amplitude shows the topography and amplitude image of the microstructure sample. The line graphs show a cross section of the images above at the position indicated by the arrow. It is clearly visible that the in the topography the slopes are steep. After each perturbation the amplitude signal is also corrected to the Set point value very quickly.

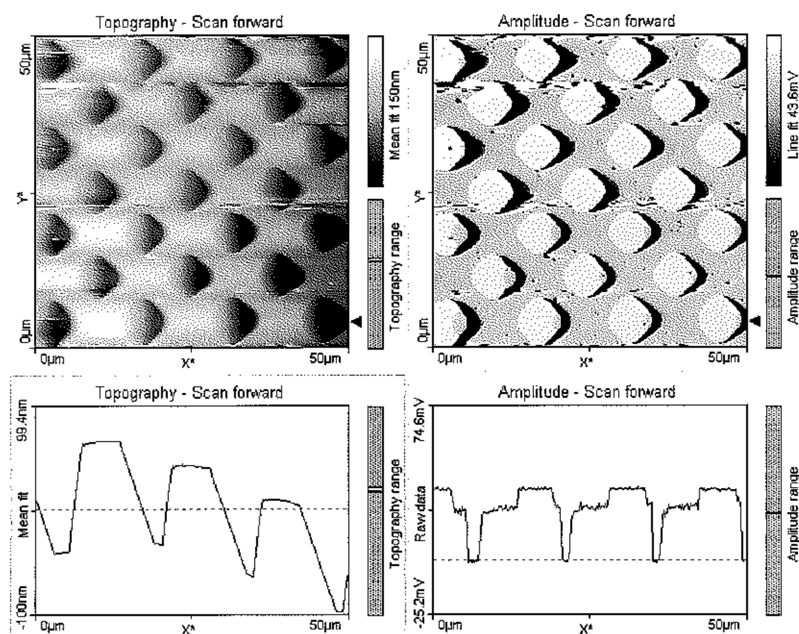

Figure 9-2: Small Amplitude. Topography and amplitude image of the microstructure sample. The line graphs show a cross section of the images above at the position indicated by the arrow. The vibration amplitude was set to 40 mV.

Figure 9-2: Small Amplitude shows the topography and amplitude image of the microstructure sample with too low vibration amplitude. The line graphs show a cross section of the images above at the position indicated by the arrow. The topography image is smeared out and the topography line graph shows a too small slope. The reason therefore can be found in the amplitude signal. The peaks are larger; this means that the correction to the amplitude to the Set point value is not as quick as in *Figure 9-1: Large Amplitude* (page 73). Due to the small vibration amplitude when the tip needs more time from the moment where it lost the contact to the surface to the moment it gains contact again. During this time the topography is uncertain and the tip is vibrating at the free vibration amplitude. Increasing the vibration amplitude or decreasing the scan speed will increase the quality again.

9.2: Microfabrication

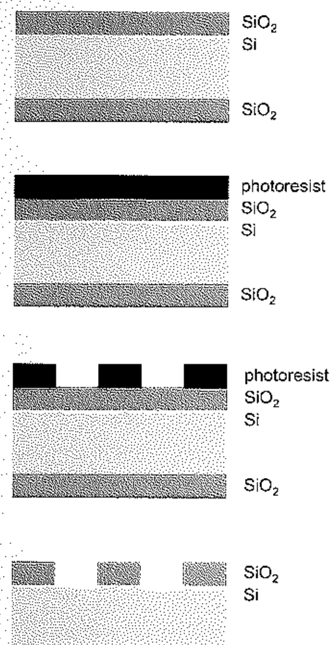

Figure 9-3: Process Flow. Fabrication process flow for the Silicon dioxide microstructures.

This sample can be fabricated with only a few steps. If you can access a clean room facility, you can easily reproduce the fabrication procedure shown in *Figure 9-3: Process Flow*:

1. Start with a plain Si wafer.
2. Make a thermal oxidation for 200 nm.
3. Spin coat the photoresist on the wafer.
4. Transfer the desired pattern to the photoresist layer by photolithography.
5. Develop the photoresist (creates holes in the photoresist layer).
6. Transfer the pattern from the photoresist layer into the silicon dioxide layer by wet etching in buffered hydrofluoric acid.

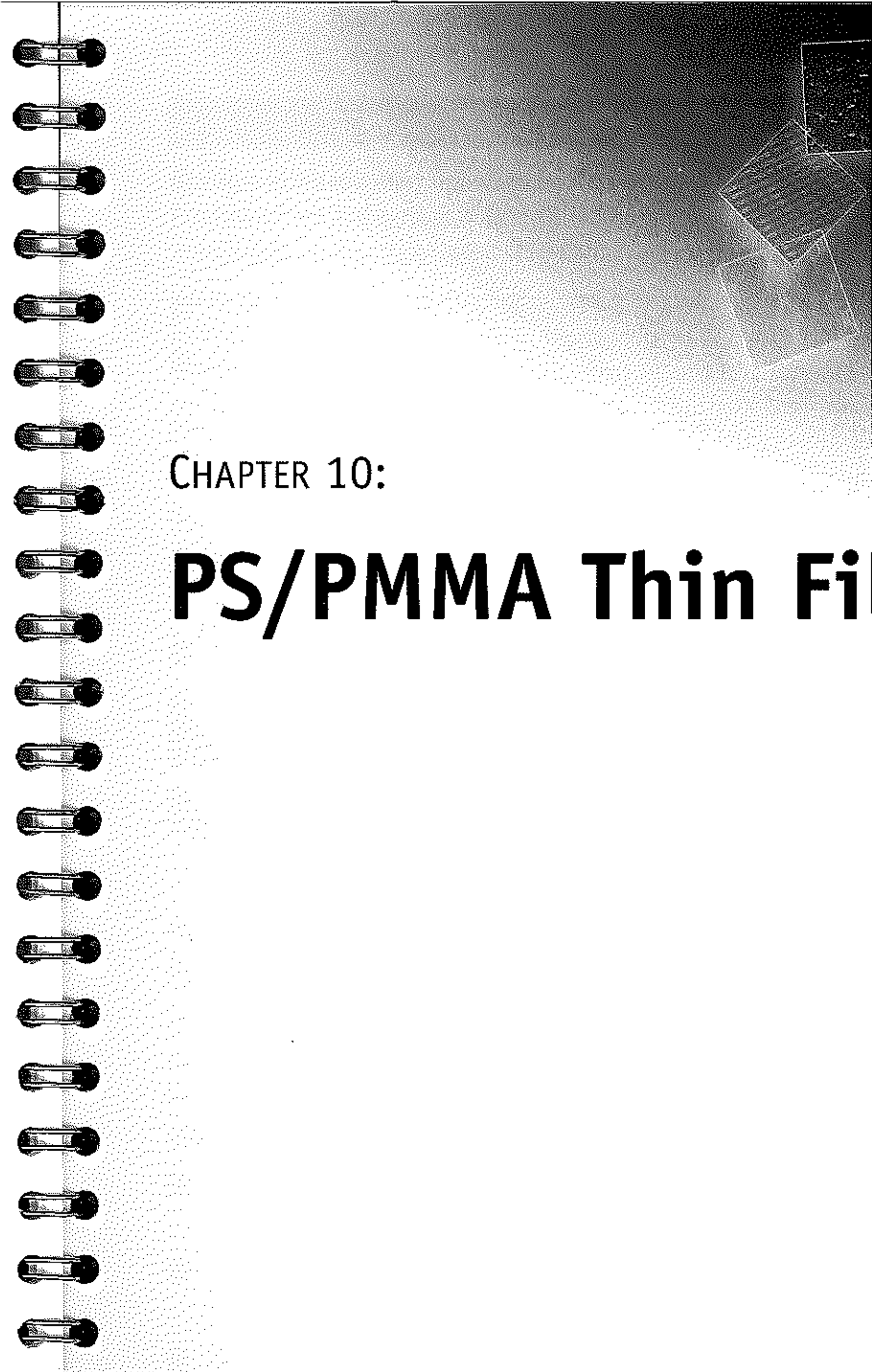

CHAPTER 10:

PS/PMMA Thin Fi

Chapter 10: PS/PMMA Thin Film

The PS/PMMA sample is a thin layer of a blend of two polymer solutions spread onto a piece of silicon wafer. Polystyrene (PS) and poly(methyl methacrylate) (PMMA), when mixed together, separate into well-defined phases on the silicon.

To prepare the PS/PMMA sample, the silicon substrate is first cleaned to make sure that it is free of large dirt. It is submerged in an ultrasonic bath in distilled water, followed by ethanol and finally propanol to perform the cleaning. Since the idea is to have an even coating of the PS/PMMA film, dirt on the silicon increases the risk of ruining the film.

To create the PS/PMMA mixture, individual solutions of PS and PMMA need to be created first. Each polymer is dissolved in toluene, a potent solvent. Then, after allowing an entire day for the polymers to properly dissolve, parts of each polymer solution are mixed together. A few drops of the mixture are placed on the piece of silicon and the substrate is spin-coated dry. Spin-coating leaves the silicon surface with only a very thin layer (film) of the PS/PMMA blend.

10.1: Measurement

10.1.1: Image Acquisition

Topography

The tip can be positioned on the entire sample. However the structure vary from region to region. For acquiring topographical images, the AFM can be operated both in static or in dynamic mode.

To start imaging sample topography:

1. Set the scan size to a maximum 10 µm.
   Due to the adhesive character of the sample, a bigger scan size will quickly wear the tip.
2. Choose an appropriate operating mode.
3. Set a small force in the setpoint.
   Choose 60% in dynamic force mode and 10 nN in static force mode.

4. Approach the sample.
   For more information on approaching the sample, see your AFM system's Operating Instructions.
5. Select a region with well-defined bumps and little to no dirt.
6. Zoom in.

Phase Contrast

If necessary, consult your user documentation on how to set up your AFM for the recording of phase contrast images.

1. Start imaging as described in *Topography* (page 78), using the Phase Contrast operating mode (an extended dynamic force mode).
2. Create a new chart in the Imaging window.
3. Select Phase Contrast to be shown in the new chart.
   Be sure to select Color Map as chart type.
4. Start a new measurement.
   Both topography and phase contrast data will now be displayed in the Imaging Window. Experiment with the amplitude to optimize phase contrast.

Lateral Force

If necessary, consult your user documentation on how to set up your AFM for the recording of lateral force images. Please note that lateral force data can only be acquired with the FlexAFM. Good results are obtained with LFMR-type cantilevers.

1. Start imaging as described in *Topography* (page 78), using the Lateral Force operating mode (an extended static force mode).
2. In addition to the Topography chart, create a new chart in the Imaging window.
3. Select Lateral Force to be shown in the new chart.
   Be sure to select Color Map as chart type.

4. Start a new measurement.

   Both topography and lateral force data will now be displayed in the Imaging Window.

10.1.2: Image Analysis

Topography of PS/PMMA

The polymer film should look like a collection of worm- or blob-like structures. The higher areas, which are the hydrophilic PMMA in a sea of PS, are 10–20 nm high. Different regions of the PS/PMMA sample may have different sized structures or heights. Close to the center of the sample, these structures have an approximate diameter of 0.1 µm. Farther to the outside of the sample, they tend to be larger. The size of the structures has (in part) to do with the amount of time that the mixed solution is allowed to rest on the silicon before it is spin-coated. The outer parts of the sample may have had more liquid solution on their surface for a slightly longer period of time than the inner regions due to the spin-coating process.

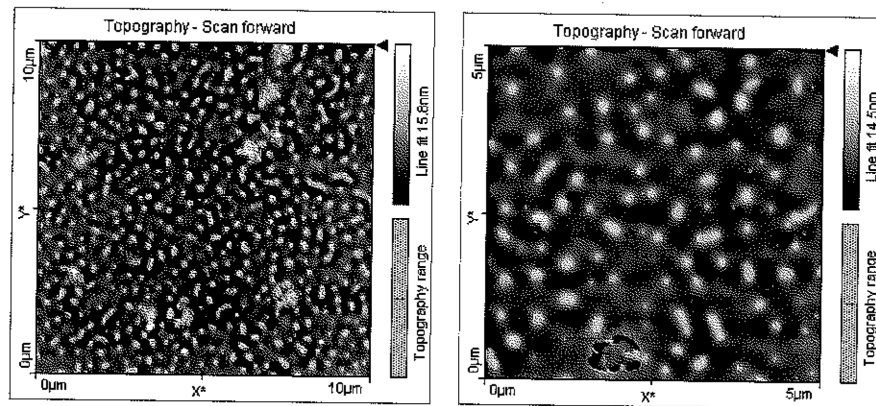

Figure 10-1: PMMA Structures Surrounded by PS. (Left) Topography with a 10-µm scan range. (Right) Topography with a 5-µm scan range. The images were recorded at the center of the PS/PMMA sample.

Figure 10-1: PMMA Structures Surrounded by PS (page 80) shows two topography frames of the polymer film. The left image has a scan range of 10 µm. In a scan range of this size, many bumps are visible, and it is possible to

locate areas without larger pieces of dirt. The image on the right is a clean area zoomed to a 5-µm scan range.

Phase Contrast of PS/PMMA

The phase contrast image gives information about the hardness of the observed sample. The PS can be discerned from the PMMA not only by topography but also by their different density. *Figure 10-2: Phase Contrast of PS/PMMA* shows a topography and phase contrast image at a 5µm scan range. The two blends are clearly discernible in both images. The Phase Contrast operating mode can thus be used to discern materials with locally different hardness, even in cases where such materials can not be identified in topography images (i.e. when they are at the same surface height). Note for example the dark areas present in the phase contrast data, which are the result of gaps in the PS layer and correspond to the underlying silicon surface. These gaps can hardly be identified in the topography data, but are clearly visible using phase contrast. Because the silicon is much harder than the softer PS and even softer PMMA, hardly any phase shift occurs over the exposed silicon areas.

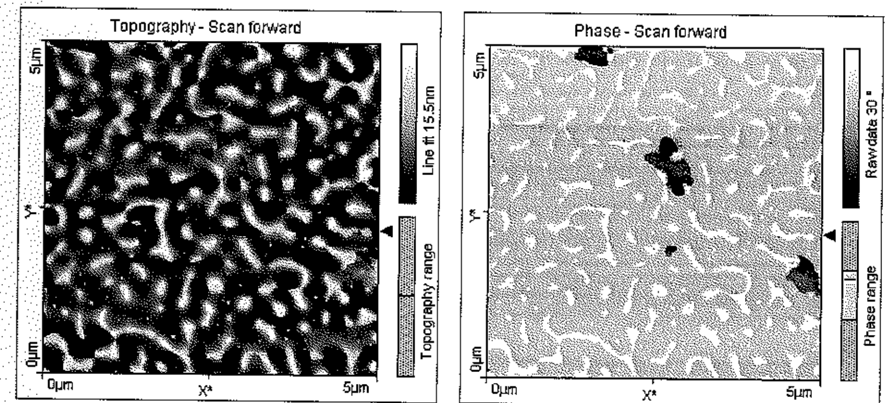

Figure 10-2: Phase Contrast of PS/PMMA. (Left) Topography of the PS/PMMA thin film. (Right) Phase Contrast of the PS/PMMA thin film.

Lateral Force of PS/PMMA

The lateral force image gives information about the lateral forces (sometimes also called friction forces) the cantilever encountered while passing over the

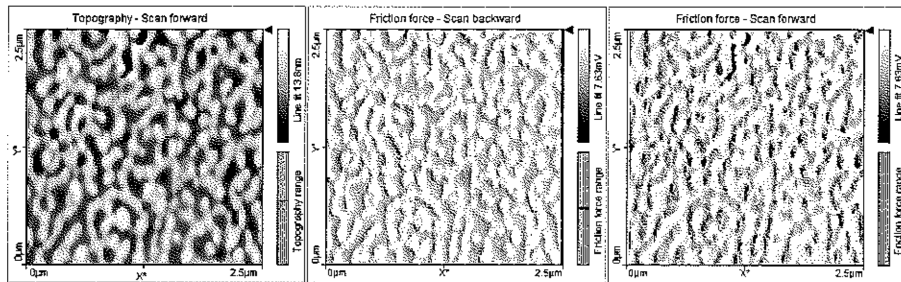

Figure 10-3: Lateral Force Measurement. (Left) Topography image with a 2.5-µm scan range. (Center) Corresponding Lateral Force image for the forward scan direction. (Right) Lateral Force image for the backward scan direction.

sample with a constant vertical force. *Figure 10-3: Lateral Force Measurement* shows the Topgraphy and Lateral Force data of the PS/PMMA sample at a scan range of 2.5 µm.

The structures seen in the topgraphy image, which correspond to the different height of the PS and PMMA (both also having different frictional characteristics due to the differences in their material properties), can also be clealrly identified in the Lateral Force images. Note the reversal of contrast in the two Lateral Force images. This reversal is the result of the sign change caused by the cantilever twisting in the other direction upon reversal of scan direction (see *Figure 10-4: Sources of Lateral Force*), and demonstrates that the lateral forces are indeed caused by differences in the materials' frictional properties. In contrast, Lateral forces caused by steep topographical features of a sample do not change sign upon reversal of the scan direction, and can thus easily be distinguished. In this sample, they do not appear to be present.

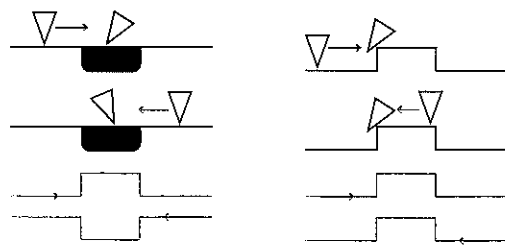

Figure 10-4: Sources of Lateral Force. (Left) Friction. (Right) Steep topography.

10.2: Relevance of Lateral Force measurements

Friction is a force that we encounter in household activity, transportation, and in industry, where any mechanical element of a machine loses energy to friction. Since atomic force microscopy uses a scanning tip in contact with a sample surface, friction forces will occur. It seems natural to want to measure the friction that is omnipresent and unavoidable. Lateral force microscopy (LFM) allows for the measurement of friction force on the microscopic level, and under the right conditions, even at the atomic level. This type of measurement is often also referred to as friction force microscopy (FFM). Studies have shown that macroscopic friction is composed of contributions of friction from many tiny contacts, which is a motivating factor for the development of LFM/FFM methods. Studies of small scale friction have shown that individual contacts do not follow the linear $f = \mu N$ relationship of macroscopic friction, and that microscopic friction force is proportional to the area of contact between substances, unlike its macroscopic counterpart.

On the atomic scale, LFM/FFM has uncovered several interesting phenomena. One such phenomenon is the so-called atomic-scale stick-slip. As the tip moves across a regular atomic surface, the lateral force increases as the tip is "stuck" in one atomic position until the force is great enough to move to the next position. The move to the next position is the "slip". As in macroscopic friction experiments, the trace and retrace signals in a stick-slip situation enclose an area on the lateral force vs. distance curve, and that this area (force times distance) is the energy dissipated in the process, allowing for the measurement of atomic scale energy dissipation.

The microscopic characteristics of friction are important since they provide a method to map interfaces of different materials in a sample, even if there are no detectable topographical features, but also because they provide explanations for the corresponding macroscopic processes. Studying the processes that contribute to macroscopic friction will contribute to our better understanding of one of the forces we encounter every day.

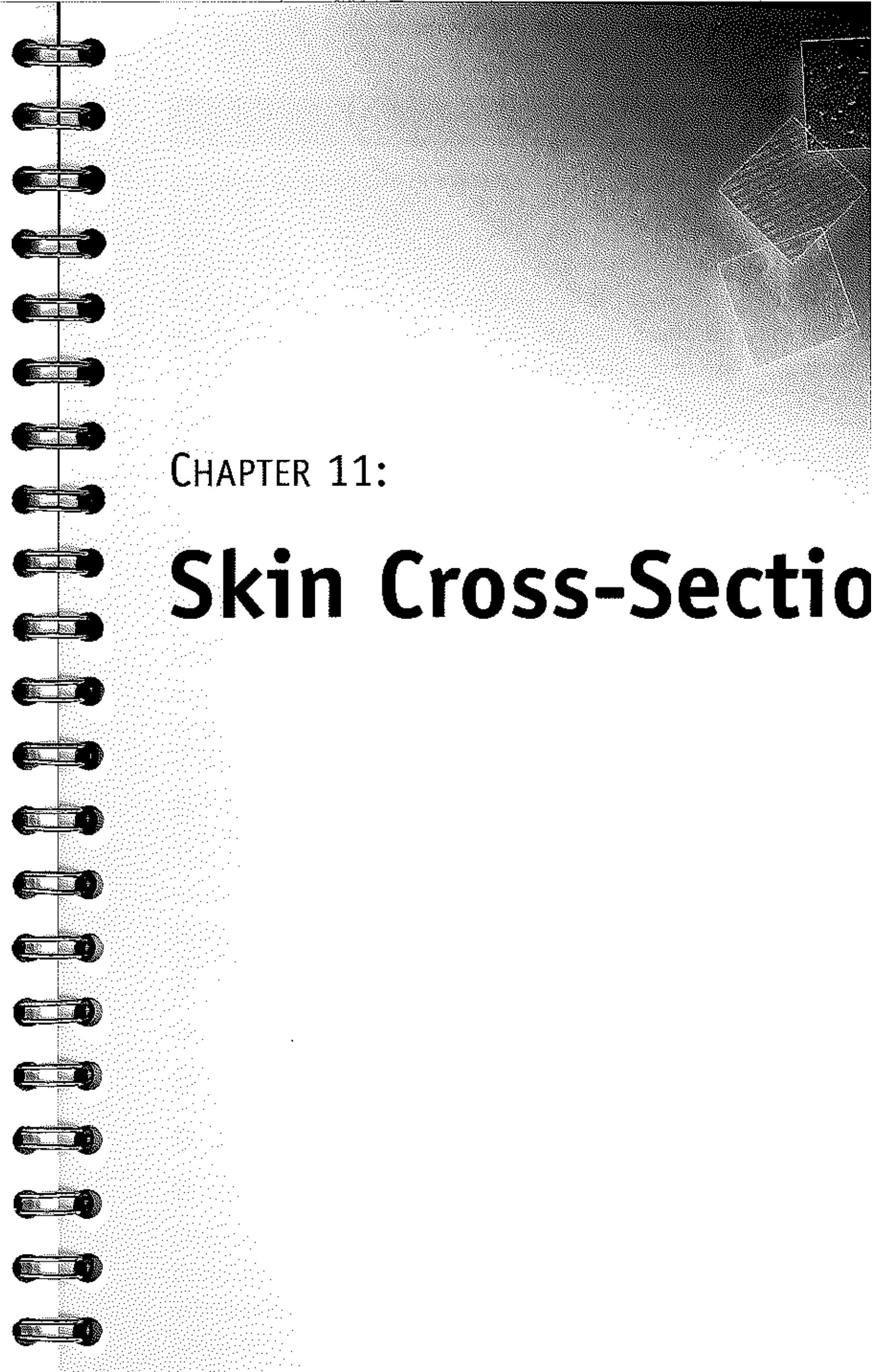

CHAPTER 11:

Skin Cross-Sectio

Chapter 11: Skin Cross-Section

This sample is typical for medical microscopy. The main application is the study the cross section of cells with high resolution.

The skin cross section sample is a thin cross section of skin, protected by plastic, and fixed to a glass slide. Move the sample back and forth in the light. You can see that at the center of the slide there is a thin curve. The entire length of the curve is the skin consecution made up various layers.

The skin sample was first fixed to the glass slide, and then dehydrated through immersion in a series of water-ethanol mixtures with increasing ethanol concentration. Next, the skin was infiltrated with and embedded in a plastic which protects the skin surface from decaying or getting dirty.

11.1: Measurement

The skin cross section is a narrow specimen which has many distinct layers and distinct structures within these layers. The specimen being narrow makes it important to line up the tip properly, to touch down on the skin as opposed to the glass slide around it. You will know if you are scanning the glass because it will appear very flat in a height scale of 100 nm, while all of the layers of skin have noticeable features in this z-range. *Figure 11-1: Skin Overview* (page 87) gives an idea of the structures that can be found within the skin.

11.1.1: Image Acquisition

In contrast to the other samples in the sample kit, the macroscopic position of the AFM tip on the sample determines what kind of structures you will see. Thus, this sample is a good sample to practice coarse positioning of the sample. Moreover the skin is hardly visible (see *Figure 11-1: Skin Overview* (page 87)).

To prepare for measurement:

1. Look at the sample under an optical microscope
2. Search some distinct features, particles or dirt
3. Memorize the position of the skin or capture the image with a camera.
4. Place the sample under the AFM

Figure 11-1: Skin Overview. The image is an overview of the skin cross section sample. The different layers are visible as well as the AFM cantilevers indicates. The image was taken with the Nanosurf easyScope 320.

5. Align the tip to the memorized position

The fact that the skin specimen has many different layers is also important in scanning, since not all of the layers will be visible in one scan range.The best strategy to see all of the structures within the skin sample is:

1. Choose a large scan range (50–100 µm)
2. Begin at one side of the skin cross section
3. Take an image
4. Retract to a safe position
5. Move slowly across the sample

Only move the sample a little bit, so as not to skip over any interesting structures. When doing this in a controlled way it is possible to assemble a mosaic of several images to a bigger one as shown in *Figure 11-3: Skin Mosaic* (page 88).

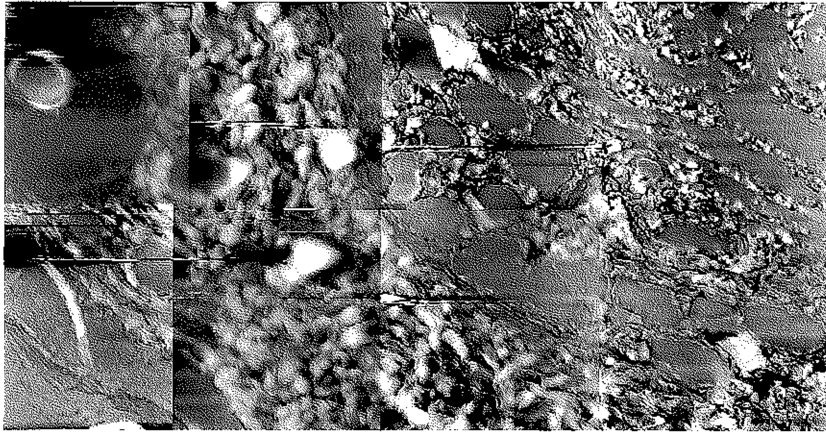

Figure 11-2: Figure 11-3: Skin Mosaic. 4x2 images with 100-µm scan rage each. The mosaic image shows a nice overview of the skin section. The images were assembled with a common image treatment software. For better results, the Stitching Module of the Nanosurf Report Expert software can be used.

11.1.2: Image Analysis

Figure 11-4: Skin Images (page 89) shows the skin images taken while moving along the cross section with the coarse adjustment.

Figure Skin Images (A) shows the outer layers of dead epithelial skin cells. The outermost layer on the right side in the image is already beginning to flake off and is much less dense than the inner layers depicted on the left. Continuing to move in the same direction across the skin will unveil deeper and deeper layers of skin.

Figure 11-4: Skin Images (B) contains multiple layers of skin. The image shows the "living" epithelial layer of skin. The structures at the bottom right hand corner of the image are the beginning of yet another layer of skin. This region is the one which contains collagen, the primary protein responsible for binding tissues within the skin.

Figure 11-4: Skin Images (C) shows a hair follicle and the structure within it. This is the hole through which actual hair would have grown. Hair follicles are quite large compared to the other structures in skin, so an entire follicle may not fit into one scan range.

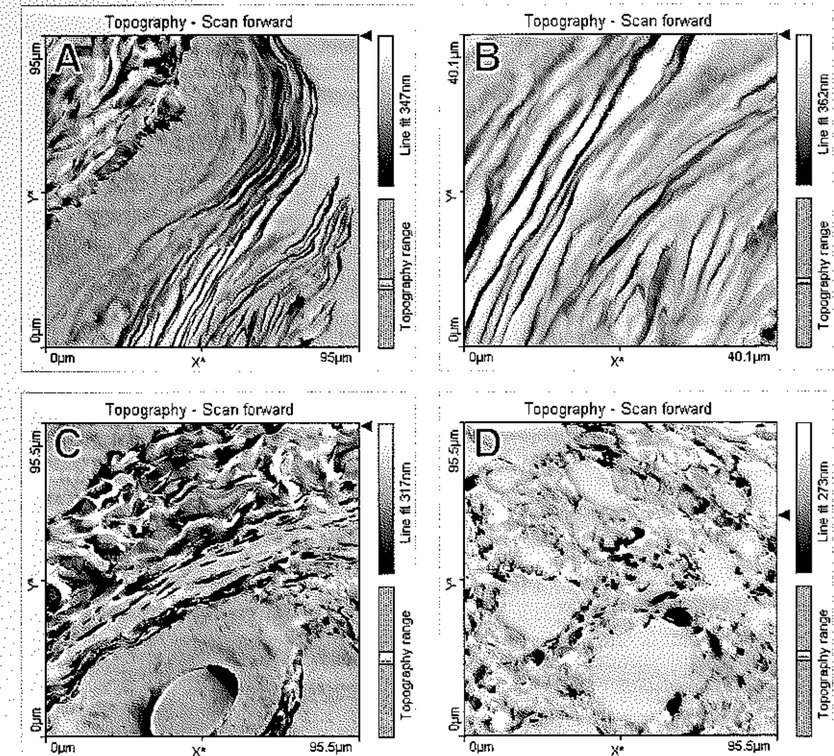

Figure 11-4: Skin Images. (A) Outer layers of dead epithelial skin. (B) Epithelial layer of skin. (C) Hair follicle. (D) Collagen layer.

Figure 11-4: Skin Images (D) shows the collagen layer of the skin section. The widely varying height of the collagen bundles makes it difficult to resolve detail on the structure of the collagen. The collagen cross sections appear circular when they run through the skin cross section, but they may not always be exactly perpendicular to the cross section of skin.

All the parts just discussed can also be seen in *Figure 11-3: Skin Mosaic* (page 88). The epithelial skin cells are in the bottom left corner, the hair follicle at the top left corner and the collagen cell on the right side of the image.

11.2: Biological Samples

Soft tissue samples can be imaged with optical microscopes, but only up to a certain resolution, and electron microscopes involve treating the sample. Even if the tissue sample is in the resolution range for optical microscopy or if it is possible to treat the sample without damaging it, these microscopes do not provide specific height information about the sample. The skin cross section in this sample was treated and is obviously not still living material. The sample shows, however, that even the soft tissue of skin can be scanned in contact mode. Atomic force microscopy gives information about the height of the structures that make up mammalian skin, even at very high resolution.

Dynamic force microscopy provides a method to explore the topography of soft tissue at a very high magnification without damaging the sample, since there is much less applied force. The fact that dynamic force microscopy can be performed with the sample submerged in solution means that skin samples (or other living samples) may be scanned without treating, or damaging them. AFM is currently being used to study DNA, RNA, proteins and individual living cells. One of the keys to studying biology is understanding that structure is related to function. The functions of certain proteins, cells, etc. are unknown, but the opportunity to explore the microscopic structure of living material offers many clues as to specific cellular functions.

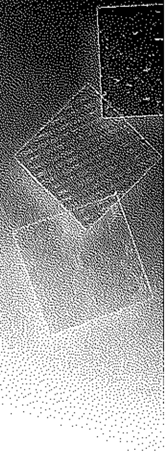

CHAPTER 12: Aluminum Foil

Chapter 12: Aluminum Foil

Aluminum foil is a common household product exhibiting interesting features on a height scale under 1µm. This sample illustrates a different way to view something that people are used to seeing on a relatively large scale. Aluminum foil is only one common household product that can be imaged with AFM to determine its microscopic structure. Other items from around the house to try imaging include: regular vs. glossy paper, hair, the Teflon coating on a razor blade, rubber, plastic, glass, metals or anything else that you can find. Not all of the items that you try will be flat enough to scan, but the ones that are may yield interesting results.

12.1: Measurements

The aluminum foil sample consists of two pieces of household aluminum foil. A sheet of aluminum foil has two sides, one more reflective than the other. One of the pieces of foil has the shiny side up; the other has the dull side up. Both pieces are glued to the sample disc.

12.1.1: Image Acquisition

The reflective side is the easier side to measure, so begin with this piece. It should be possible to see the cantilever's reflected image in the shiny piece of aluminum.

The diffuse side provides no usable mirror image of the cantilever. Instead, you can use the shadow of the cantilever, which is however not as easily visible.

To image the aluminum foil:

1. Approach the cantilever to the sample using its reflected image or shadow.
2. Continue until the two are close but do not yet touch each other.
   See the *AFM operating instructions* for more information on how to approach samples
3. Start automatic approach.
4. Measure the reflective and diffusive sample.
5. In order to compare the two measurements, set the color map height scale to identical values in both measurements.

12.1.2: Image Analysis

Reflective Side

Figure 12-1: Reflective Side Overview shows an image taken of the reflective side of the foil, seen in both height and surface views. The most noticeable feature in this figure is the set of parallel lines of varying height running across the image. These lines extend for very long stretches along the foil. Try scanning at the maximum scan range of your microscope. You should find that the lines extend for this entire scan range. Another feature of the sample topography is the set of pits that are lower down that the average height level. These pits are visible as dark spots that in the bright lines running from the bottom to the top of the color map chart.

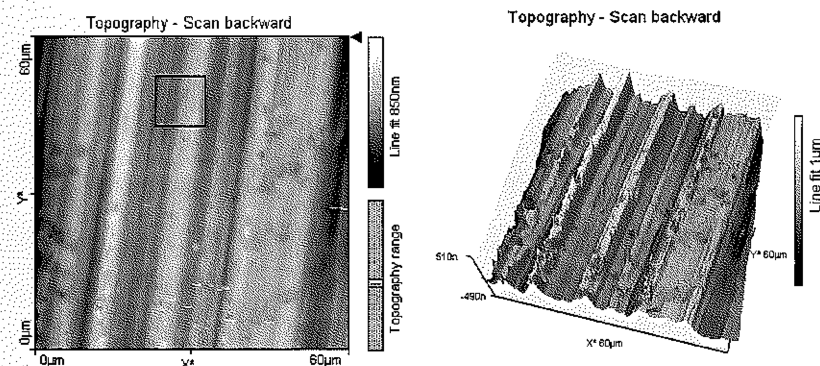

Figure 12-1: Reflective Side Overview. Measurement with in a scan range of 60 µm. (Left) Color map chart with a height scale of 850 nm. (Right) 3D view (projection).

The two charts in *Figure 12-1: Reflective Side Overview* complement each other by highlighting slightly different information. The height image points out the well-defined lines of different height, while the three-dimensional surface view gives a good idea of the transition between the higher and lower regions. For example, the height image makes it clear how deep the pits are, but not how steep the drop from the surrounding area into the pit is. The color map better illustrates this.

Figure 12-2: Detail of Reflective Side shows a zoomed measurement on the area indicated in *Figure 12-1: Reflective Side Overview* (page 93). All images show the same area, the image on the left was measured in the same orientation as the overview; the other images are measured in a 90 degrees rotated direction. In the image on the left, the lines of different height are well defined and quite large. The image in the center shows the same area, measured at 90 degrees rotation. In both the left and center image, the mean height of each line is subtracted before displaying the image. Due to this data processing, the center image clearly shows that the larger lines are composed of smaller lines with less height contrast on a smaller scale, and the holes in the surface become very conspicuous. To show that both the left and the center data actually display the same structure, the image on the right shows the same measurement without data processing.

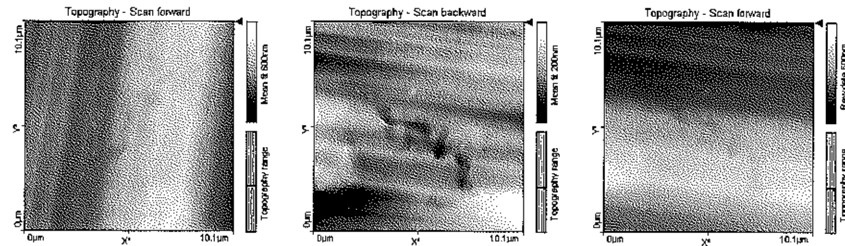

Figure 12-2: Detail of Reflective Side. Aluminum foil in a scan range of 10 µm. (Left) 0 degrees scan rotation, mean fit processed data. (Center) 90 degrees scan rotation, mean fit processed data. (Right) 90 degrees scan rotation, raw data. The orientation of the scan direction with respect to the features in the sample can make a huge difference when data processing is used on the image.

An interesting analysis to perform on this sample is a section analysis. A section running perpendicular to the lines of different height can help to determine the height differences between adjacent lines, as well as the maximum height difference between the highest and lowest points in the line selected. *Figure 12-3: Reflective Side Cross Section* shows the section analysis of a line running through the lines of different height on the shiny side of the aluminum foil. The line selected runs through one pit, which is visible as a dip in the sectional cross section chart. The Measure Length tool is used to measure the half width (705 nm) and depth (50 nm) of the pit.

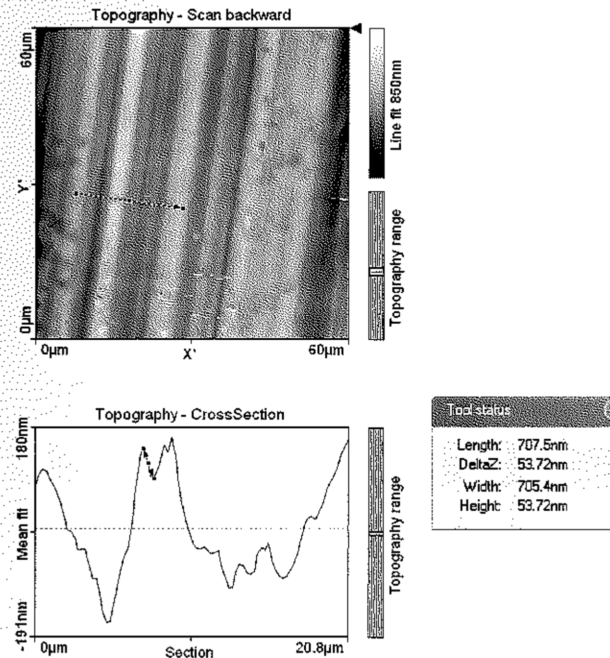

Figure 12-3: Reflective Side Cross Section. Analysis of the overview measurement.

Diffuse Reflective Side

On inspection of the measured surfaces, such as shown in *Figure 12-4: Comparison* (page 96), it immediately becomes clear that the diffuse reflection of the surface is due to its much rougher and more irregular surface. There appear to be lines running from the top of these images to the bottom, but the lines are not as well-defined or as thin as those on the reflective side of the foil. There are pits in the diffuse reflective side as well, but they appear less deep, and more elongated than on the reflective side. Additionally, whereas the pits on the reflective side are mainly located on bright (i.e. high) lines, here they seem to run parallel to the smudged lines. To further analyze the dull side of the foil, attempt a section analysis. You should find that the shiny side is between two and three times as flat as its non-reflective counterpart.

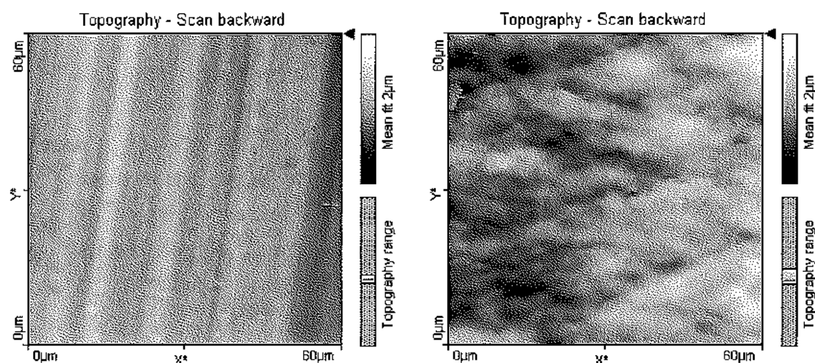

Figure 12-4: Comparison. (Left) Reflective side. (Right) Diffuse reflective side.

12.2: Bulk Foil Production

Commercially available aluminum foil generally has one side different from the other. The two pieces of aluminum foil in this sample are representative of these different sides.

The lines across the foil and the craters spread throughout it are consequences of the rolling process that renders the foil flat and shiny. Aluminum is mined, refined and processed into large sheets. Initially, the sheets are quite thick (close to 1 cm), and they must go through several rolling procedures until they are flat enough for use as foil. Foil is loosely defined as a sheet of thickness less than or equal to 100 µm, and most foils are somewhere in the range of 5 to 75 µm. The foil in this sample is approximately 30 µm thick. Generally, two sheets of a thicker aluminum foil are rolled together at the same time to save time and energy. The two sheets are rolled one on top of the other with oils or other lubricant between them, as well as between the foil and the rollers, as shown in *Figure 12-5: Foil Production.* Thus, the two sides of the foil are exposed to different conditions during the rolling process.

The reflective side of the foil was in contact with a harder surface (the roller), it is flatter and shinier. The non-reflective side is only in contact with another sheet of aluminum foil (another non-reflective side), and so is less flat and reflective. The lines of different height on the shiny side of the foil are a result of the rollers

pushing into the foil, so the lines run in the same direction as the length of the roller, as depicted in *Figure 12-5: Foil Production.*

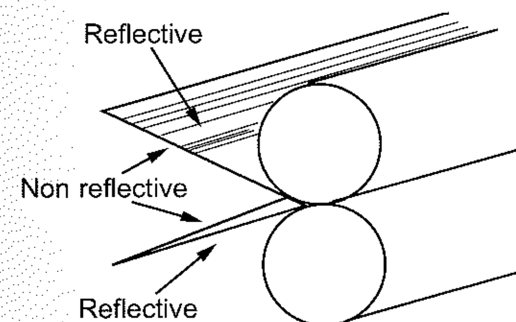

Figure 12-5: Foil Production. The process that leaves one side of the aluminum foil shinier than the other side.

The pits, seen in the various measurements are caused by the oil placed between the rollers and the foil to prevent overheating. The oil gets trapped between the roller and foil, and is forced down since it has no other place to go.

12.3: Sample Maintenance

Of all the samples in the Sample kit, the aluminum foil sample is the only one that can hardly be damaged by cleaning. To clean the sample, drop some ethanol onto the aluminum foil, and wipe it dry with a clean paper tissue.